



Long-term Creep-Fatigue Interactions in Ni-base Superalloys

**Award DE-FE0011722
August 2013 – August 2016
Program Manager: Briggs White**

PI: Richard W. Neu

GRAs: Ernesto Estrada, Liang He, Michael M. Kirka, Sanam Gorgan Nejad

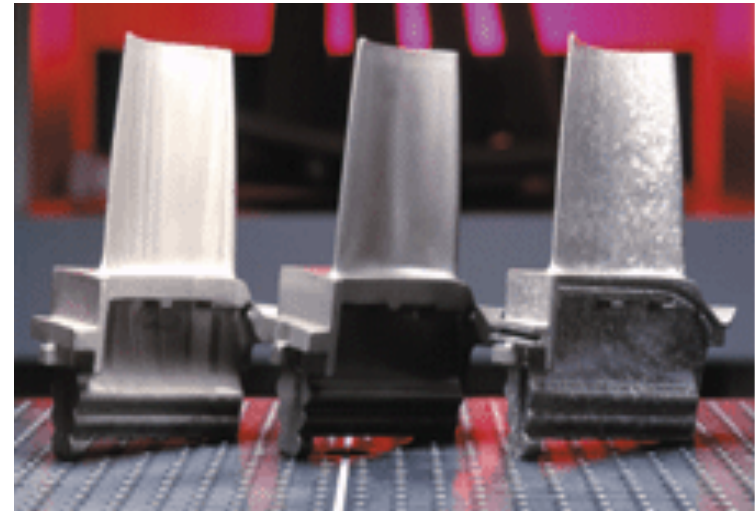
**The George W. Woodruff School of Mechanical Engineering
School of Materials Science & Engineering
Georgia Institute of Technology
Atlanta, GA 30332-0405
rick.neu@gatech.edu**

**University Turbine Systems Research Workshop
Purdue University
October 21-23, 2014**



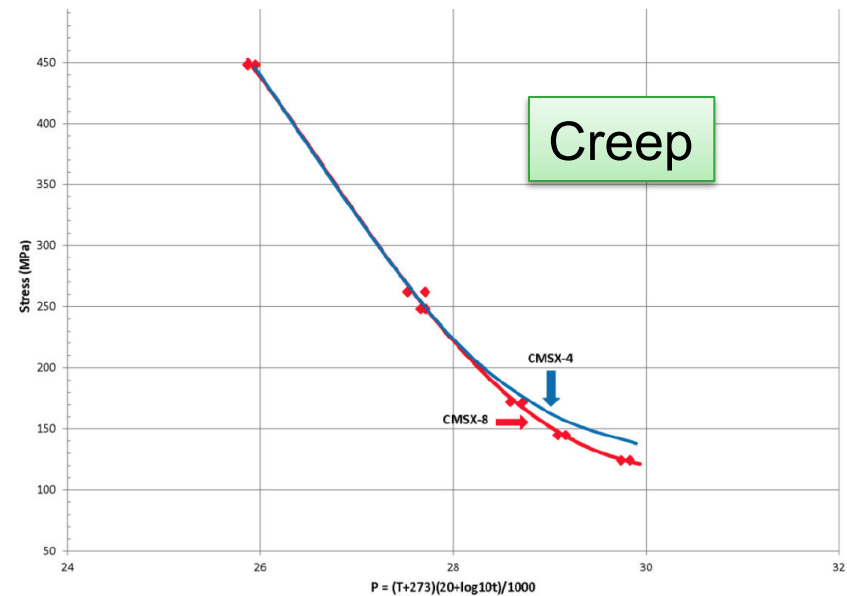
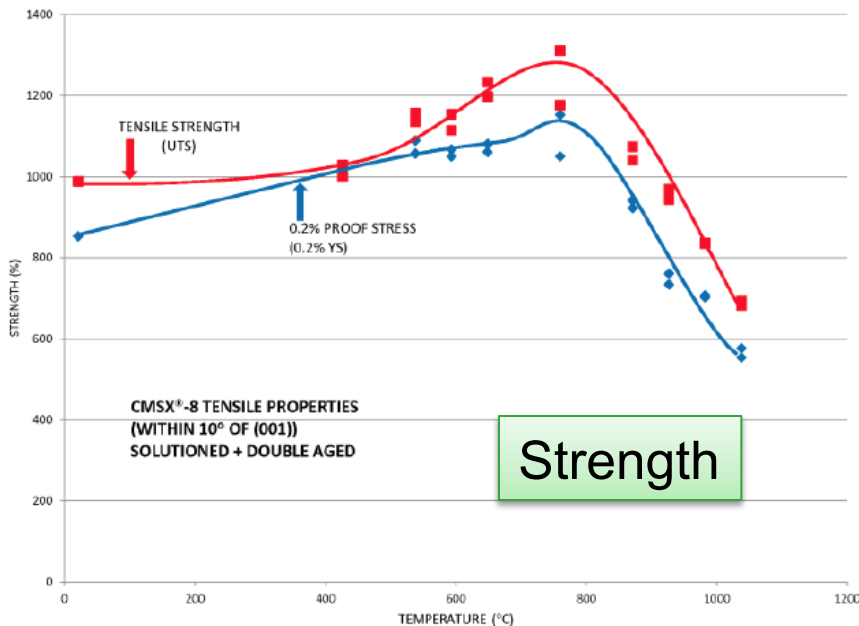
Land-based gas turbines

- drive to increase service temperature to improve efficiency; increase life
- replace large directionally-solidified Ni-base superalloys with single crystal superalloys

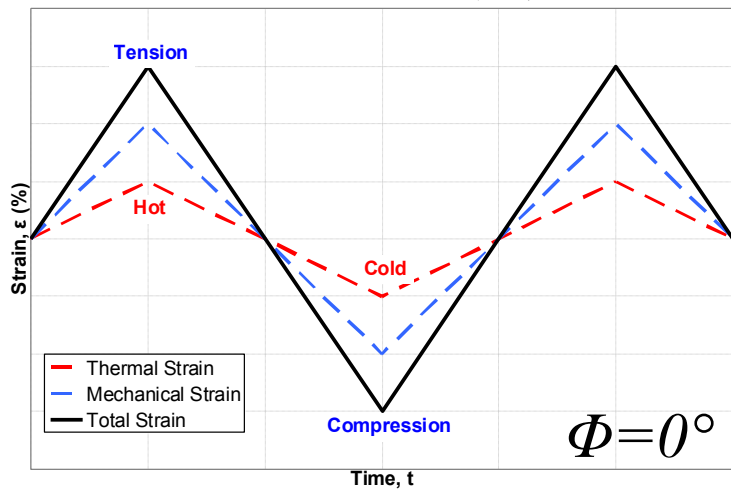


CMSX-8: 1.5% Re "alternative 2nd gen alloy" replacing 3.0% Re containing alloys (e.g., CMSX-4, PWA1484)

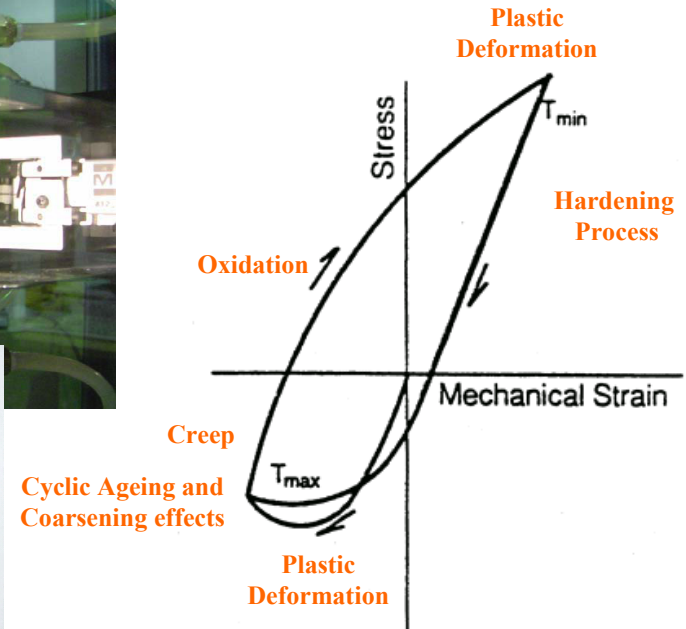
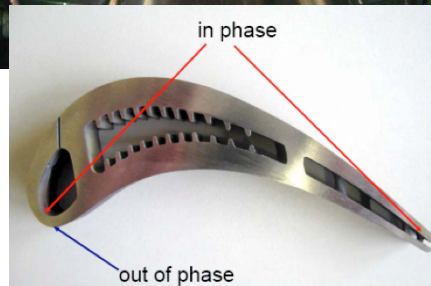
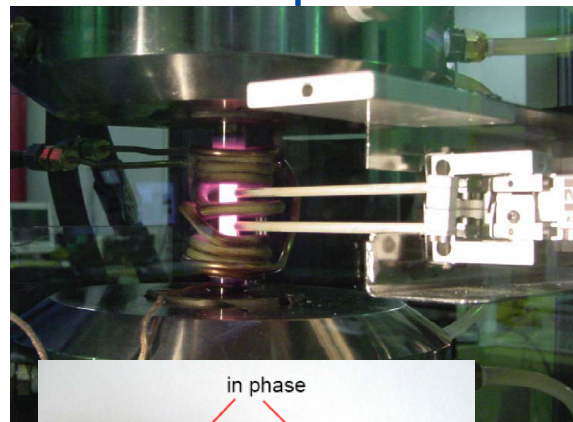
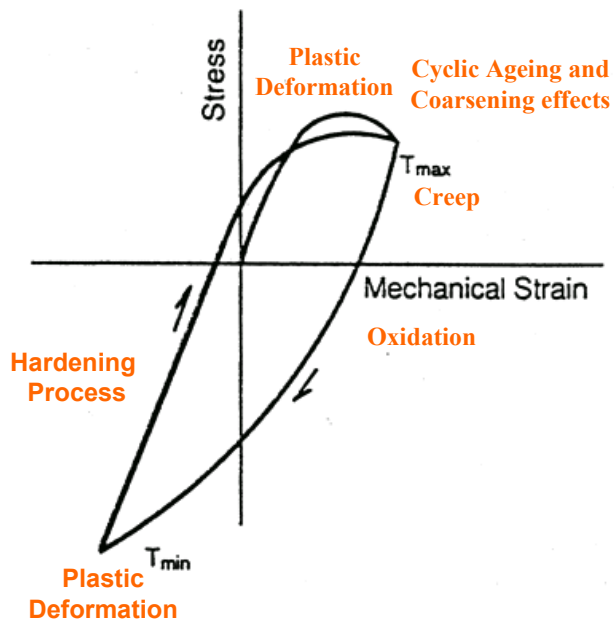
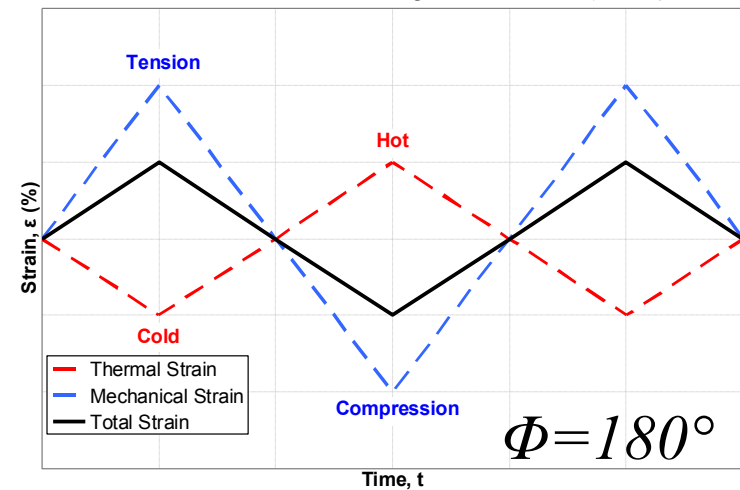
Alloy	Cr	Co	Mo	W	Al	Ti	Ta	Re	Hf	C	B	Zr	Ni
Mar-M247LC-DS	8.4	10.0	0.7	10.0	5.5	1.0	3.0	-	1.5	0.07	0.015	0.05	Bal
CM247LC-DS	8.1	9.2	0.5	9.5	5.6	0.7	3.2	-	1.4	0.07	0.015	0.01	Bal
CMSX-4	6.5	9.0	0.6	6.0	5.6	1.0	6.5	3.0	0.1	-	-	-	Bal
SC16	16	0.17	3.0	0.16	3.5	3.5	3.5	-	-	-	-	-	Bal
PWA1484	5.0	10.0	2.0	6.0	5.6	-	9.0	3.0	0.1	-	-	-	Bal
CMSX-8	5.4	10.0	0.6	8.0	5.7	0.7	8.0	1.5	0.2	-	-	-	Bal



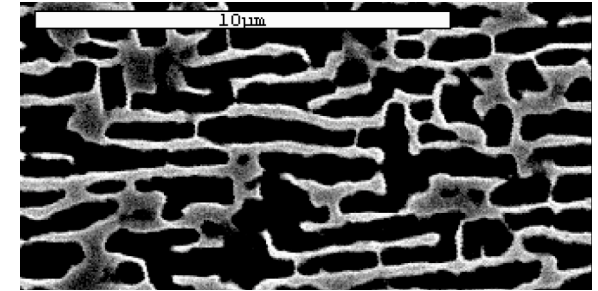
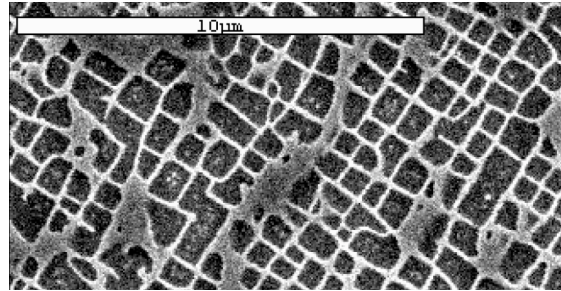
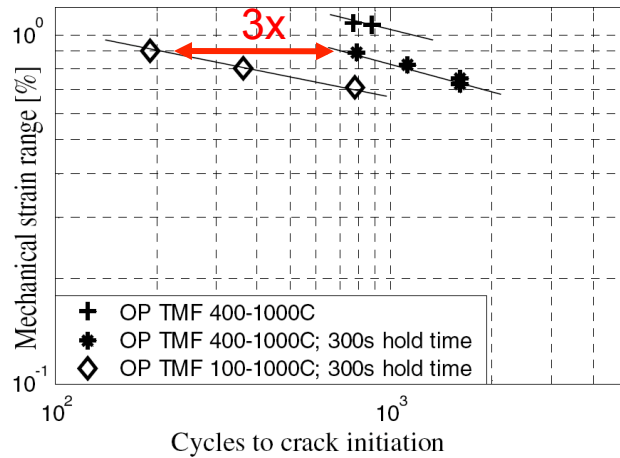
Linear In-Phase (IP)



Linear Out-of-Phase (OP)

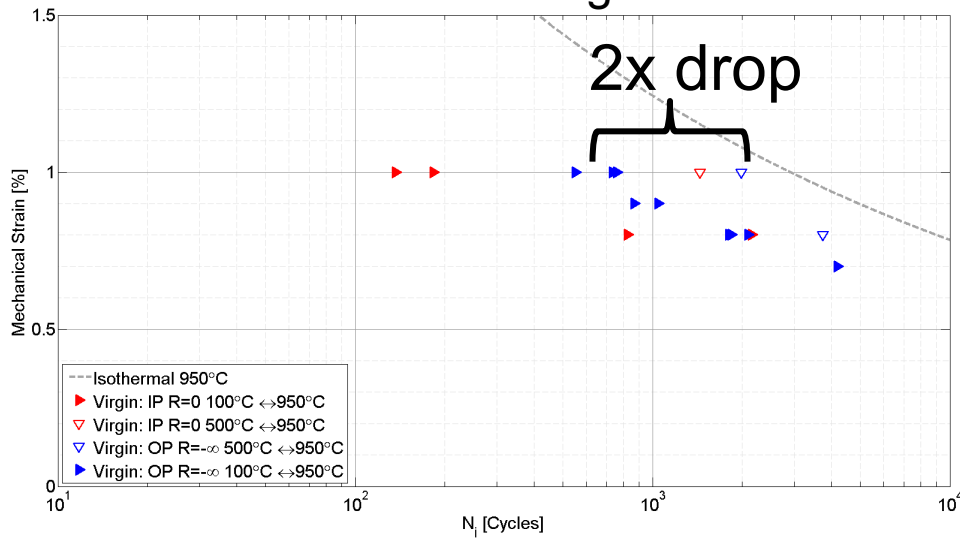


CMSX-4 [001]

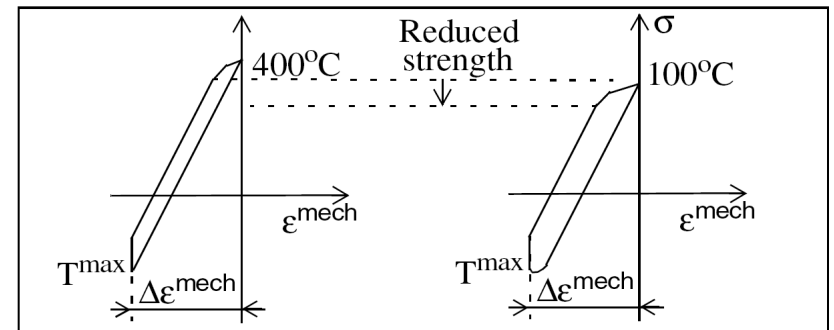


[Arrell et al., 2004]

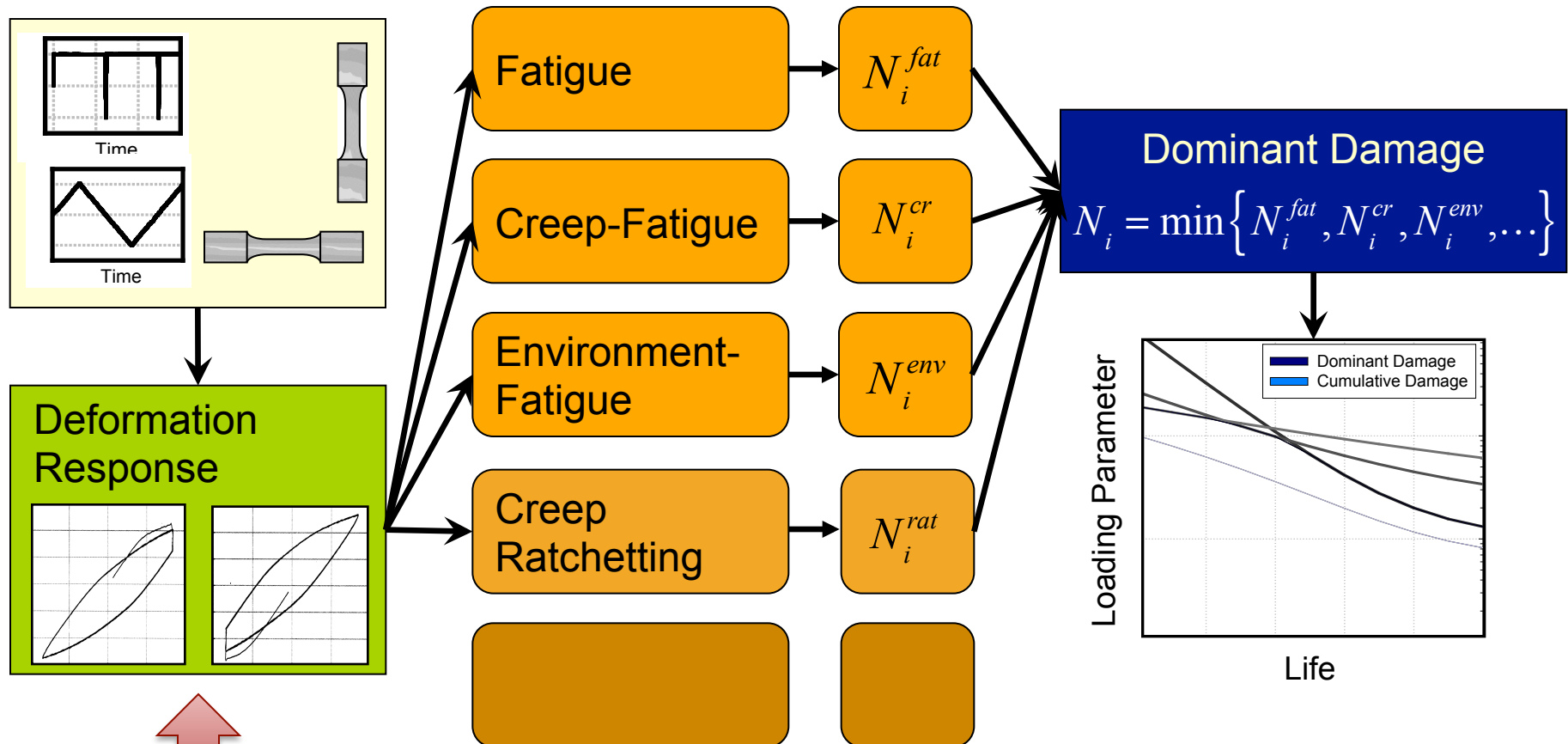
CM247LC DS in Longitudinal Dir.



[Kirka, 2014]



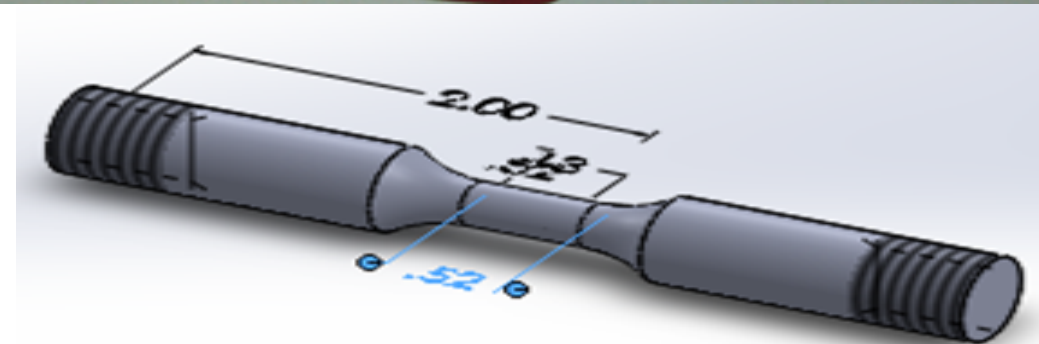
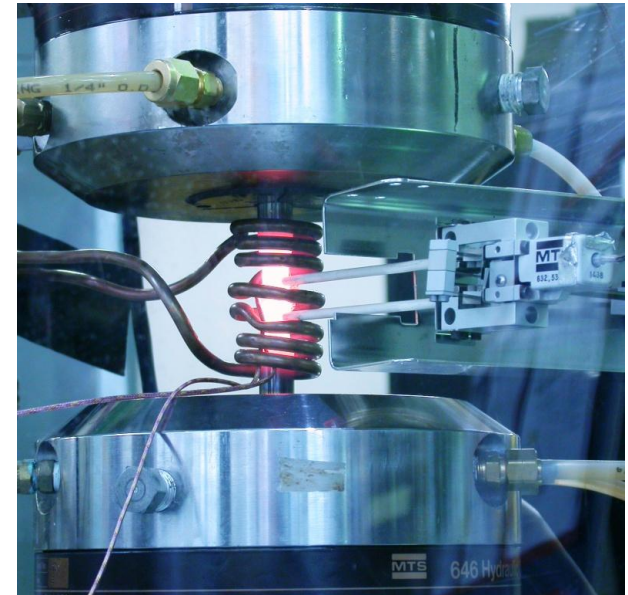
Damage Mechanism Modules

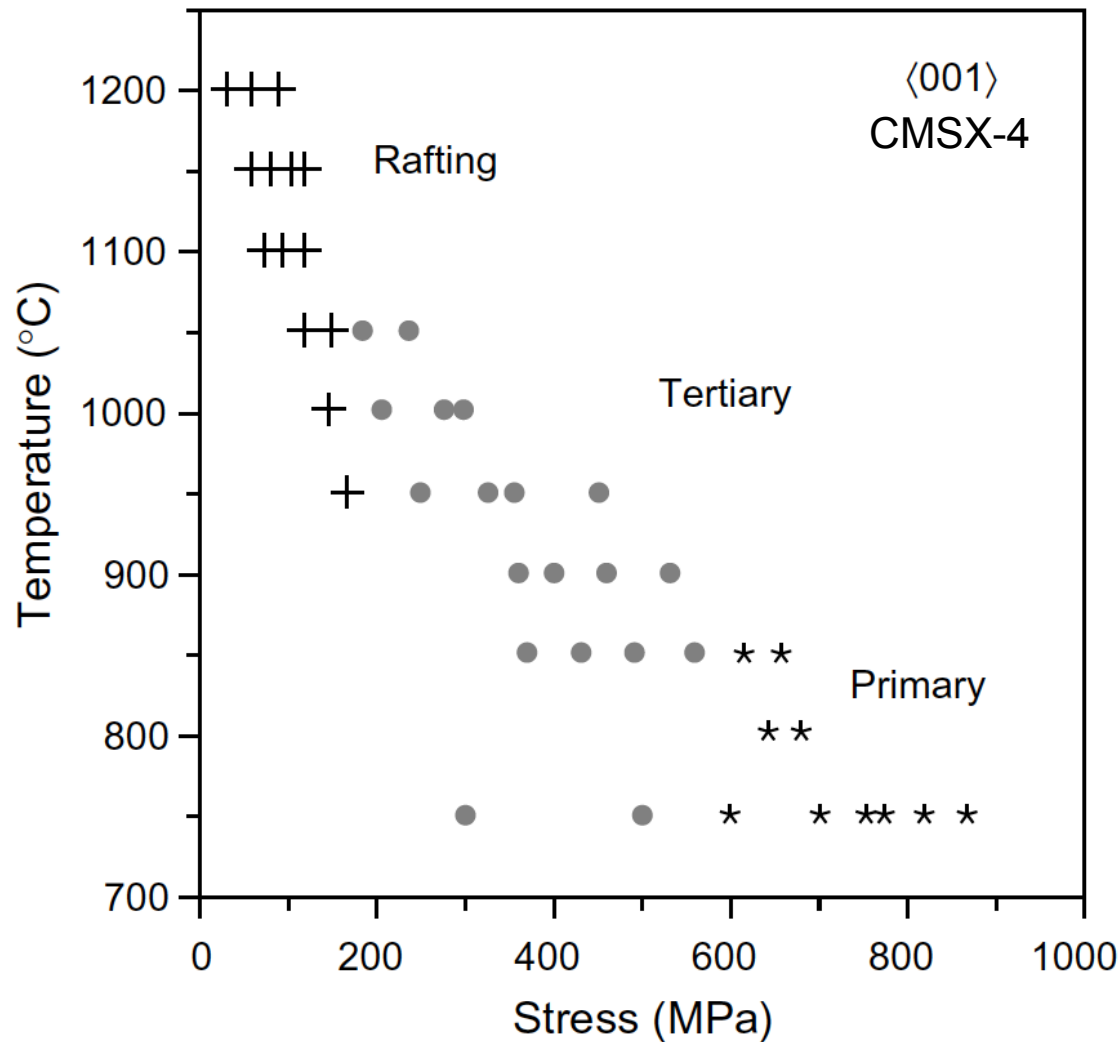


Accurate representations of the deformation response highly critical for predicting crack formation

- Creep-fatigue interaction experiments on CMSX-8
- Aging studies and influence of aging on creep-fatigue interactions
- Crystal viscoplasticity to capture the deformation response

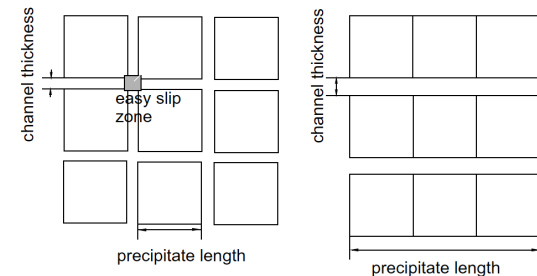
- Conventional creep-fatigue (baseline)
 - ASTM E2714-09
- Long-term creep followed by fatigue
- Fatigue followed by long-term creep
- Impact of pre-aging
- Creep-fatigue interaction life analysis
- Orientations: $\langle 001 \rangle$, $\langle 111 \rangle$, $\langle 011 \rangle$
- Application to TMF with long dwells



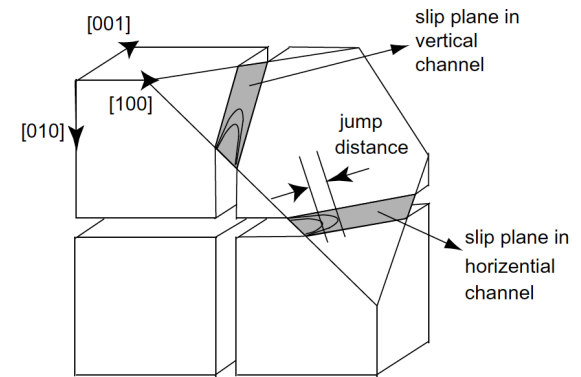


[Reed, 2006; Ma, Dye, and Reed, 2008]

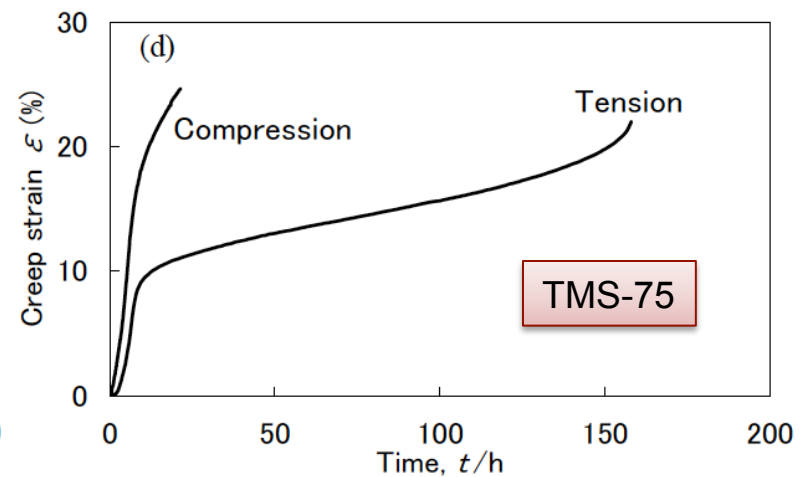
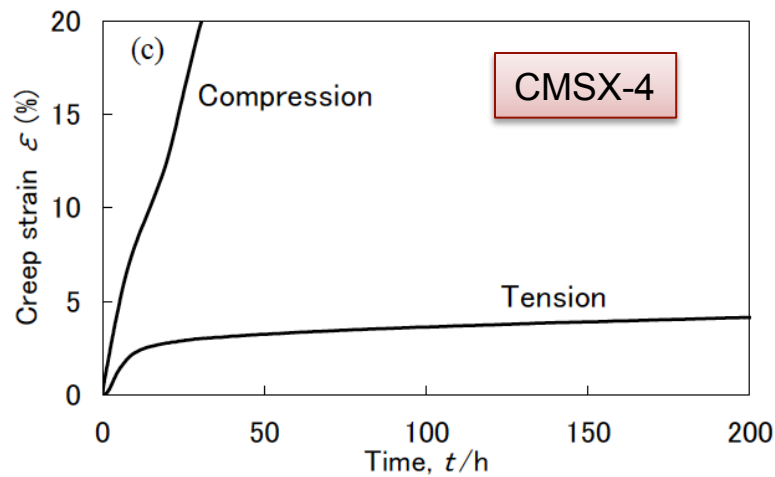
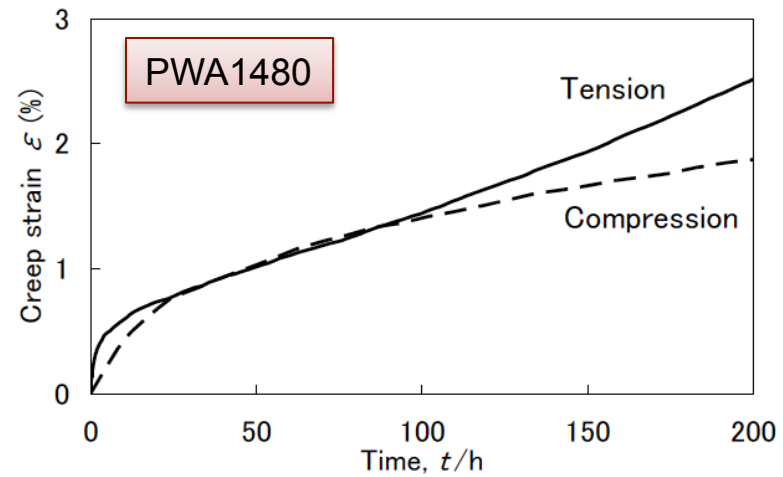
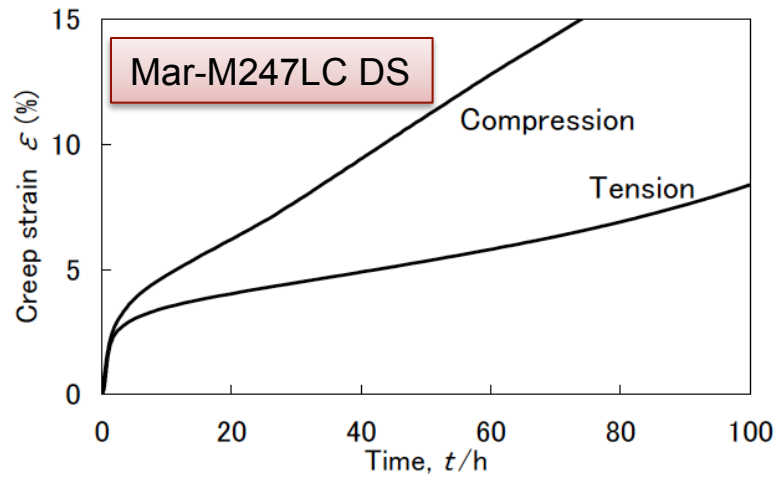
Rafting – transport of matter constituting the γ phase out of the vertical channels and into the horizontal ones (tensile creep case)



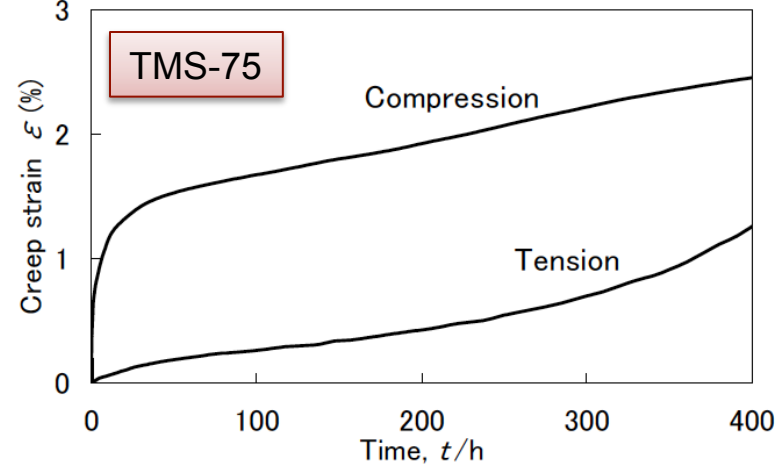
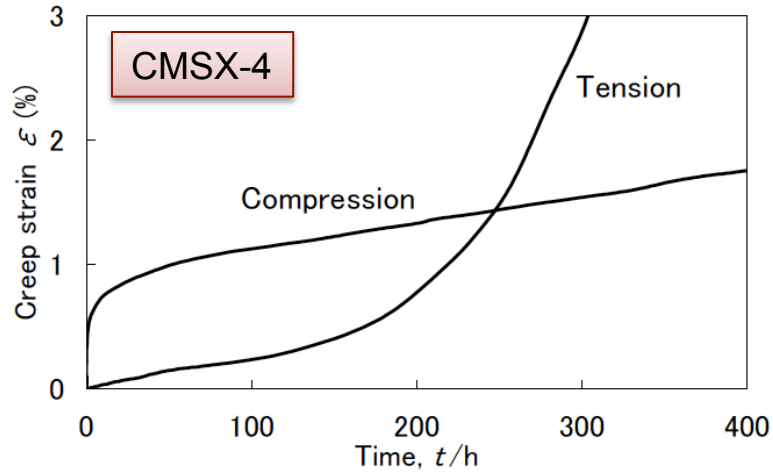
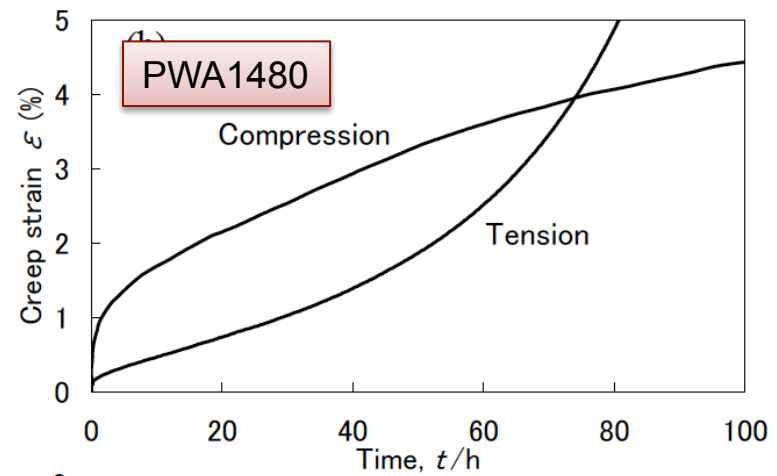
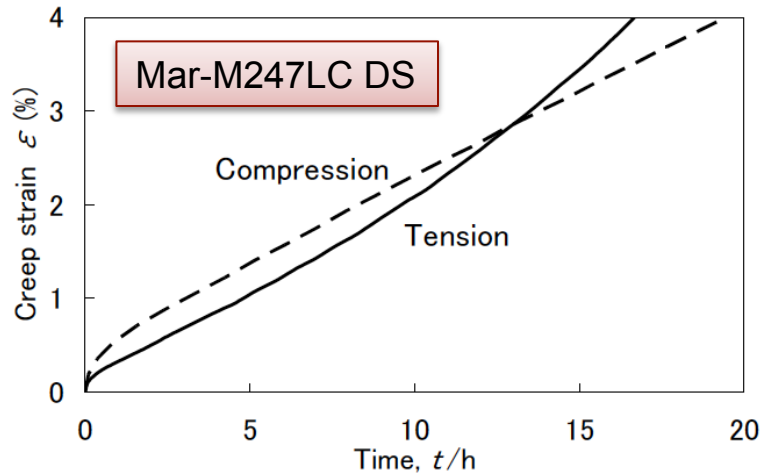
Tertiary – dislocation activity restricted to $a/2\langle 110 \rangle$ form operating on $\{111\}$ slip planes in the γ channels



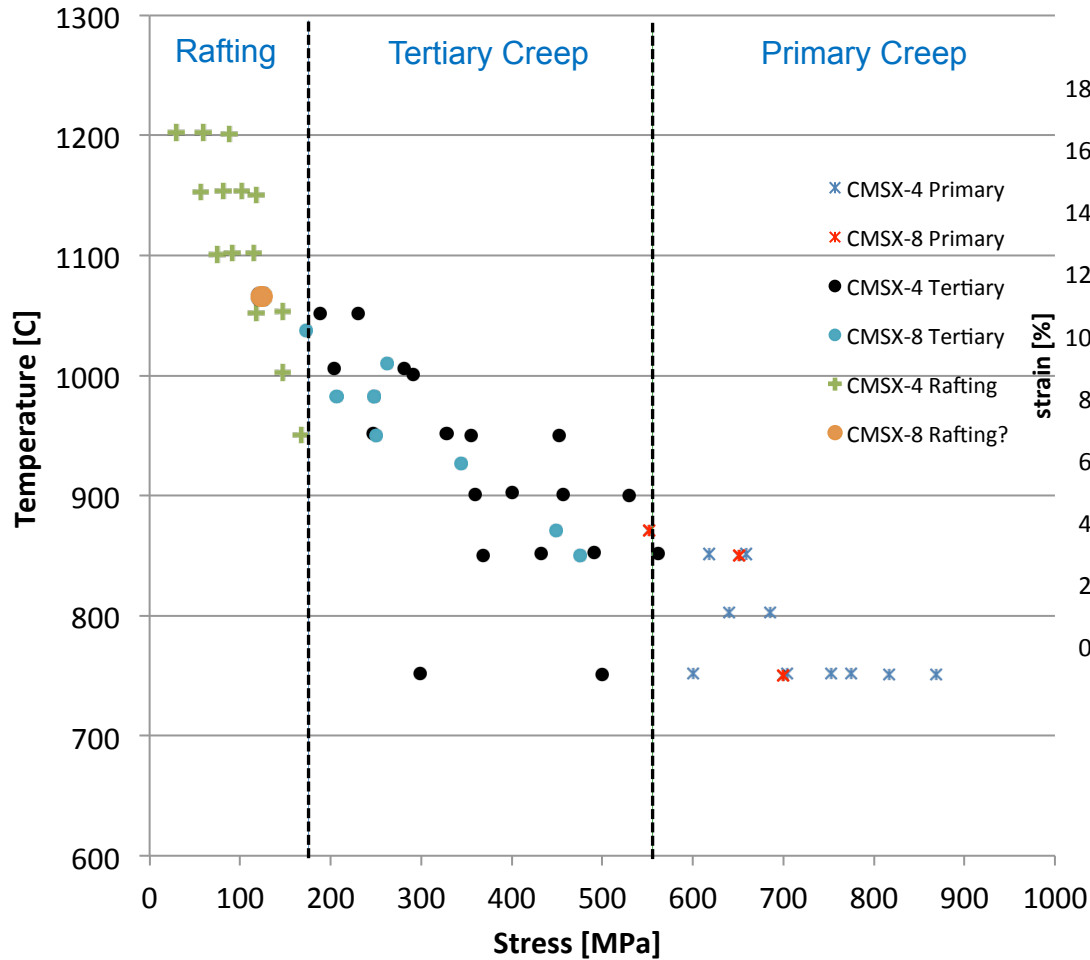
Primary – γ' particles are sheared by dislocation ribbons of overall Burgers vector $a\langle 112 \rangle$ dissociated into superlattice partial dislocations separated by a stacking fault; shear stress must above threshold stress (about 550 MPa – uniaxial normal stress)



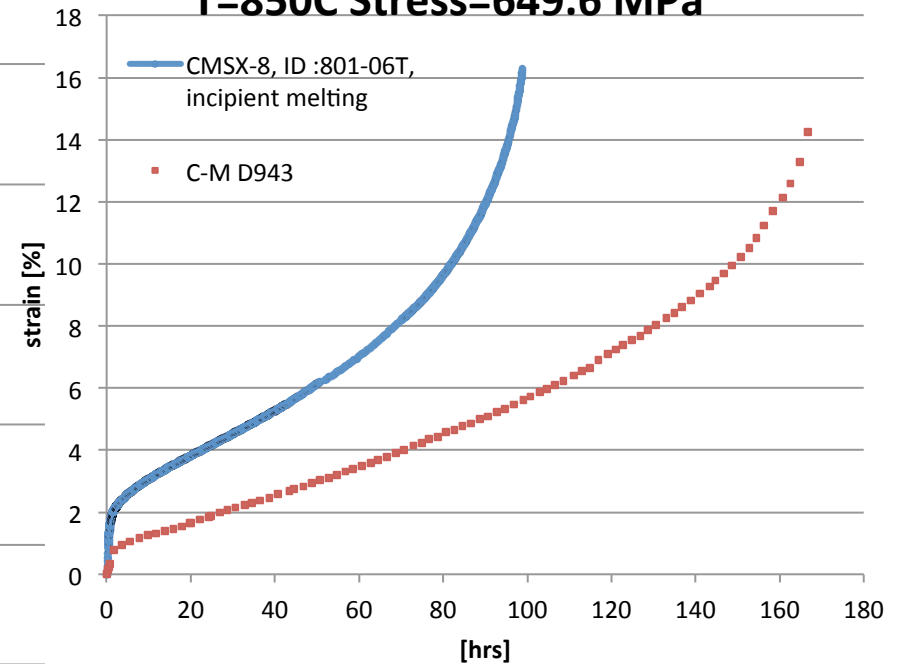
Note: Primary Creep Regime (based on tension)



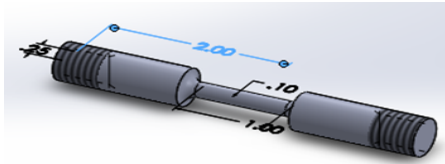
Note: Tertiary Creep Regime (based on tension)



Virgin CMSX-8 Specimen 80106T
T=850C Stress=649.6 MPa

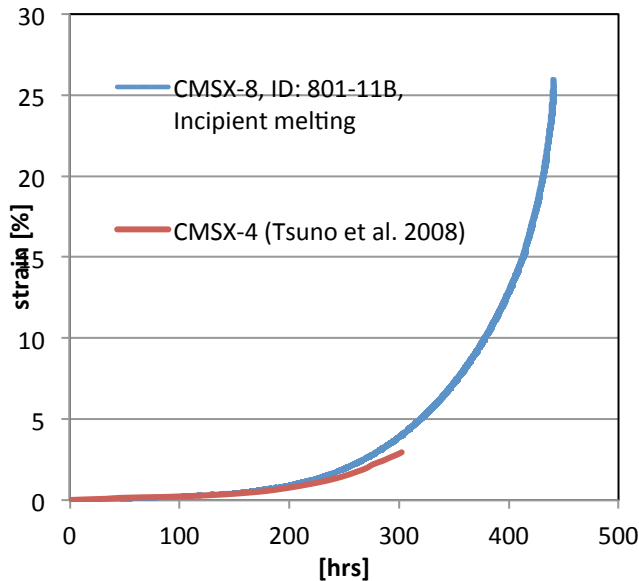


- LMP = 24.70
- Life to rupture = 98.90 hrs.
- Temp = 850 C
- Stress = 650 MPa
- Alpha = 4.1



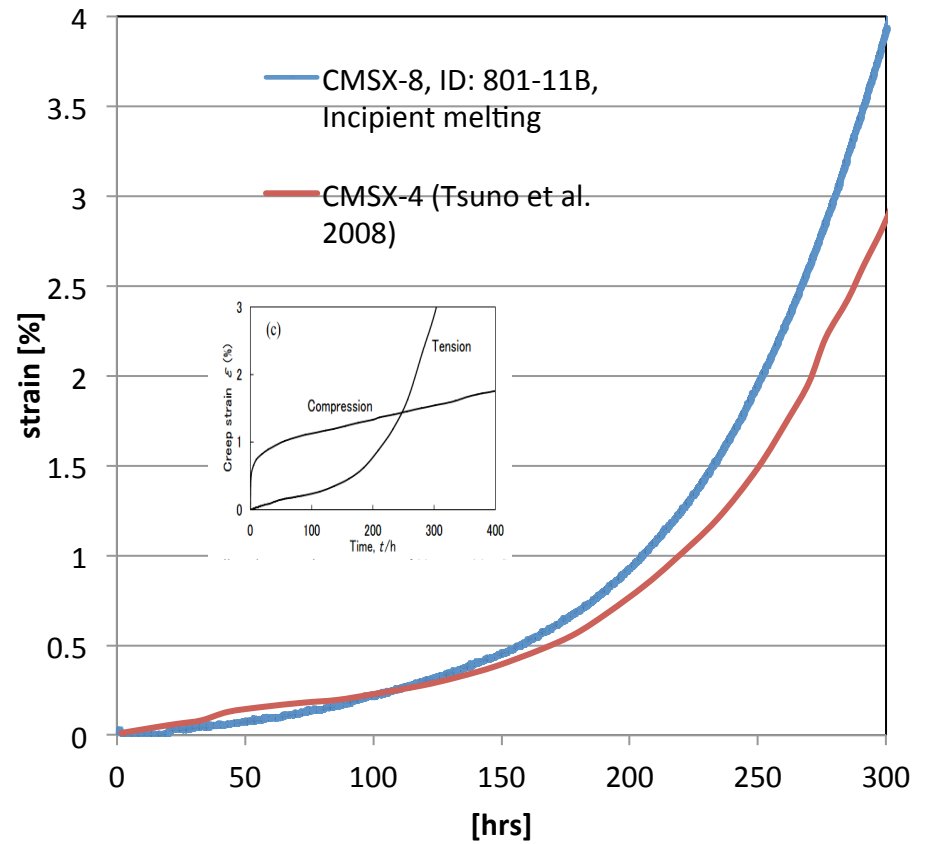
801-11B

Virgin CMSX-8 Specimen 801-11B
T=900°C Stress=392 MPa

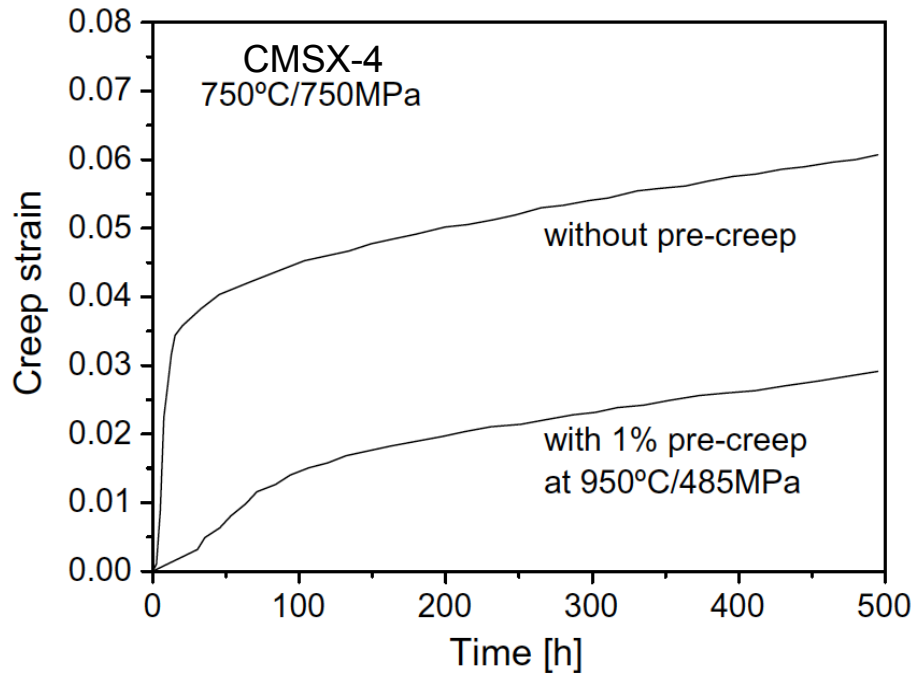


Zoom-in

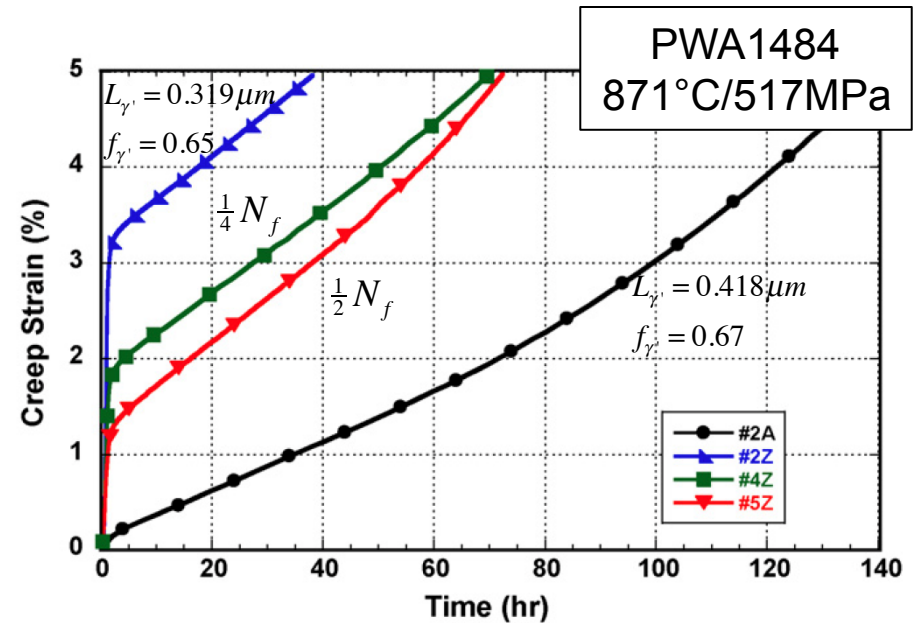
Virgin CMSX-8 Specimen 801-11B T=900°C
Stress=392 MPa



- LMP=26.57
- Life to rupture = 451.78 hrs.
- Temp = 900 C
- Stress = 392 MPa
- Alpha = 5.8



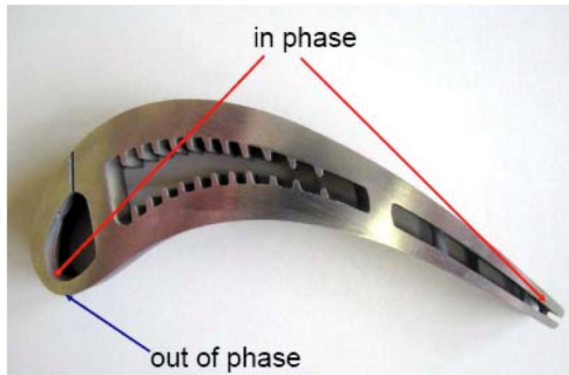
[Ma, Dye, and Reed, 2008]



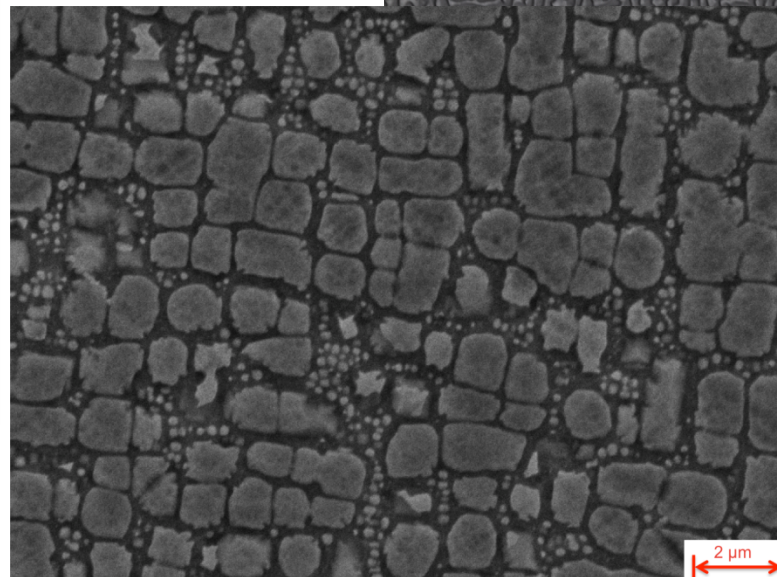
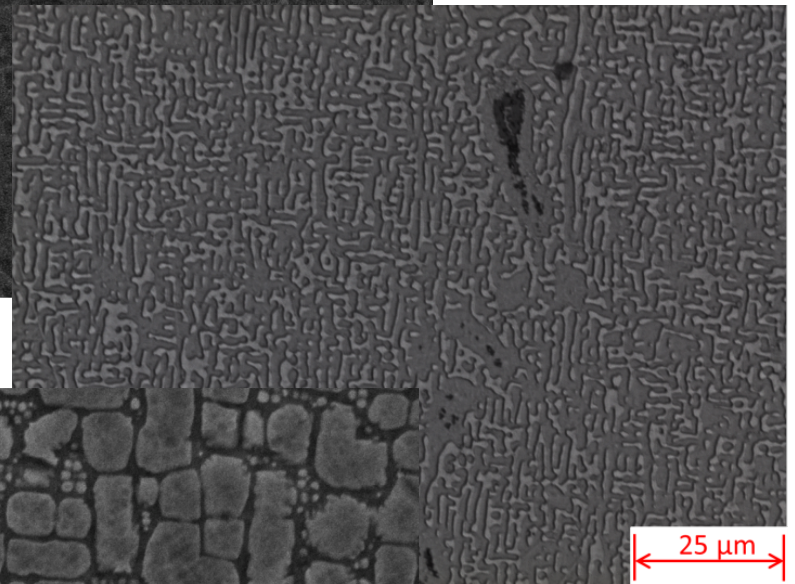
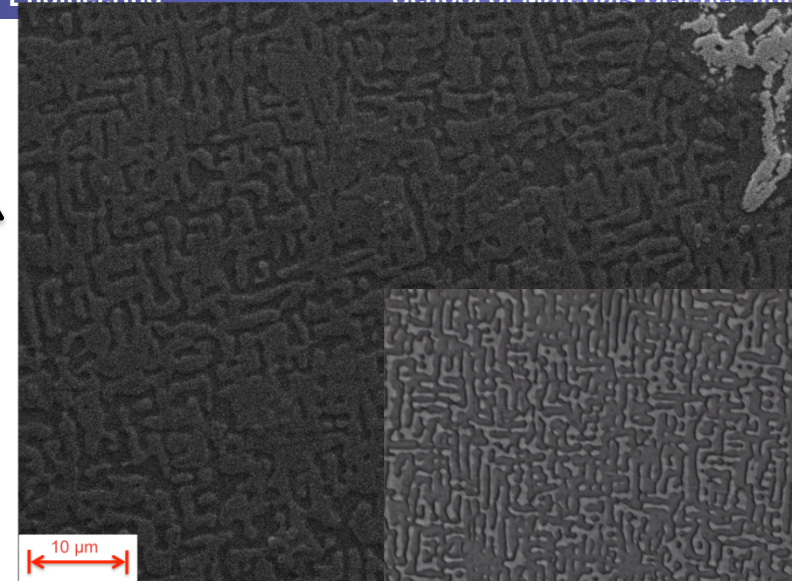
[Pierce, Palazotto, & Rosenberger, 2010]

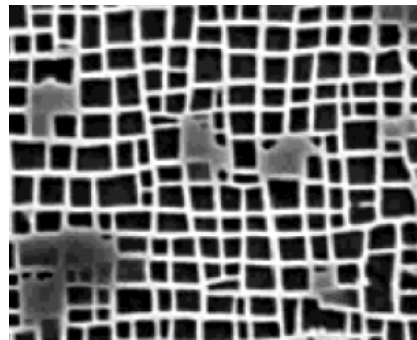
PWA1484 exposed to 871°C for 32 hrs
also reduces primary creep

[Wilson & Fuchs, Superalloys 2008]

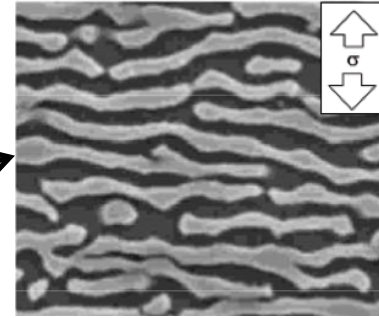


Distance from Root

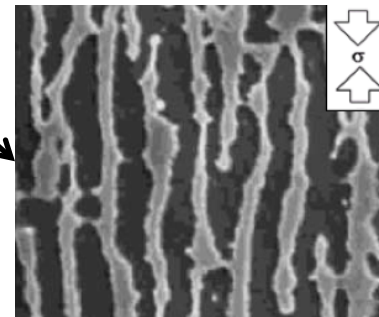




Tension
Compression

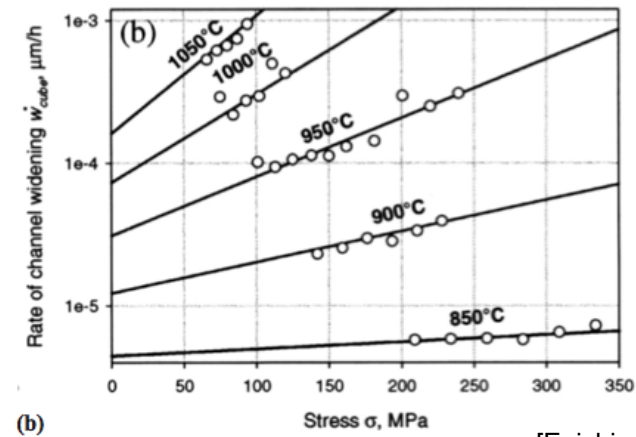
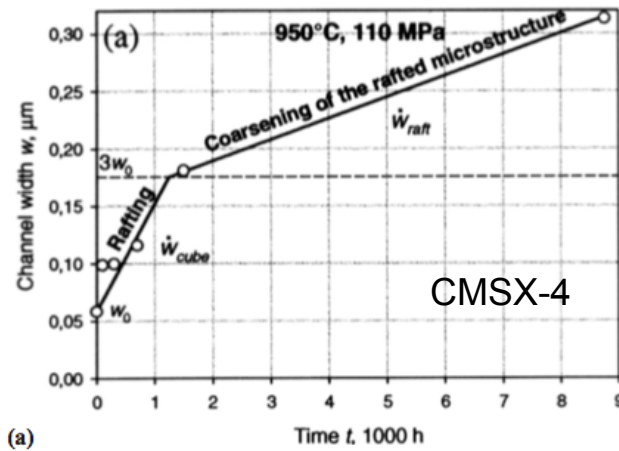


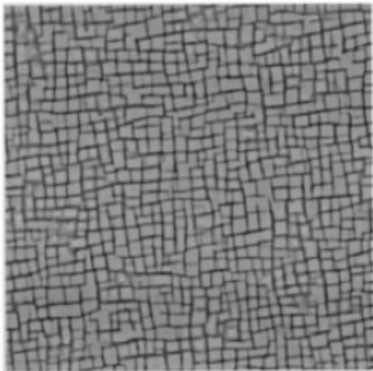
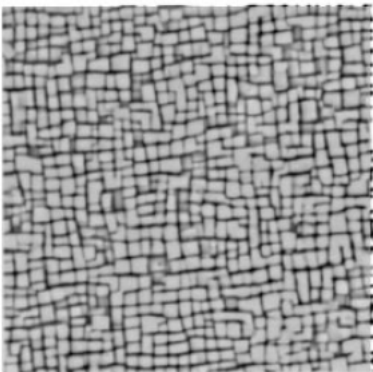
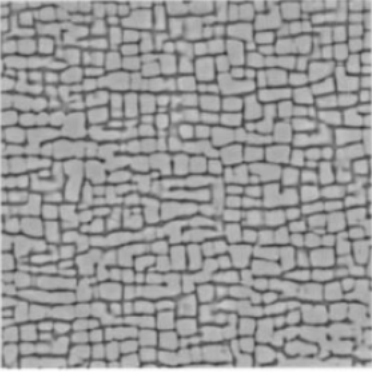
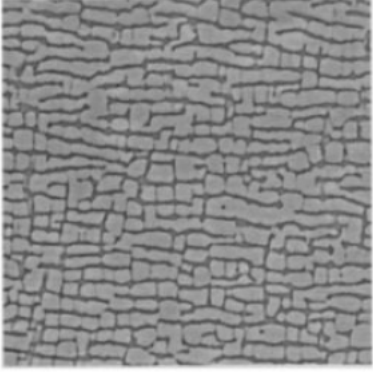
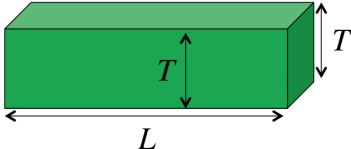
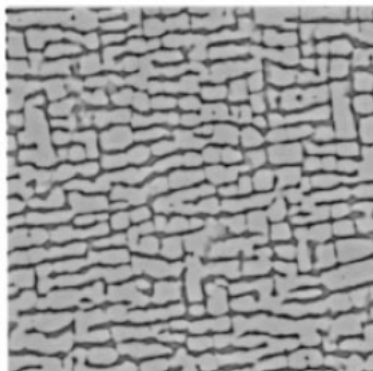
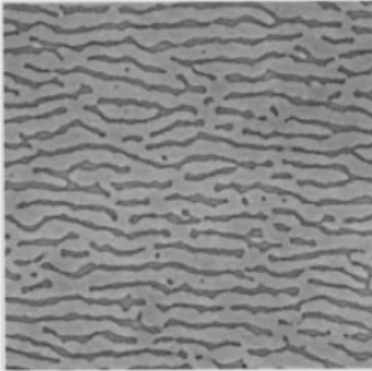
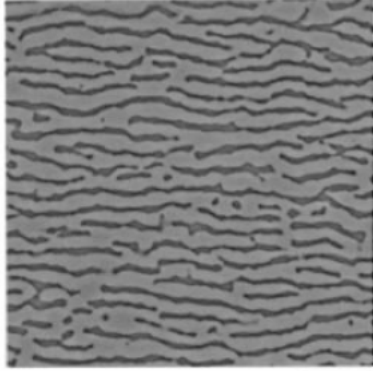
N-raft



P-raft

$$\delta = \frac{2(a_{\gamma'} - a_{\gamma})}{a_{\gamma'} + a_{\gamma}}$$

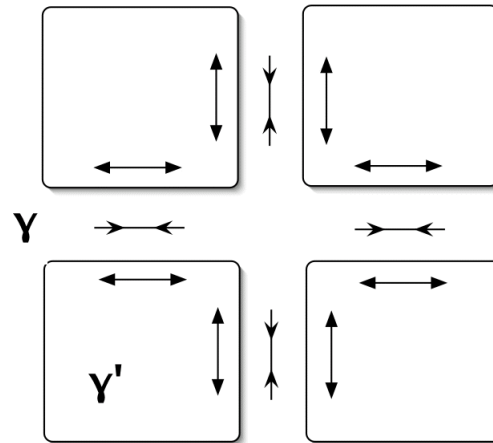


Initial	A: time=150 Hours strain=0.06% R=0.55	B: time=280 Hours strain=0.07% R=0.69	C: time=550 Hours strain=0.27% R=0.94
<p>CMSX-4</p> 			
$R = \frac{L}{2T}$ 	<p>D: time=695 Hours strain=0.13% R=1.07</p> 	<p>E: time=1060 Hours strain=1.06% R=1.28</p> 	<p>F: time=1170 Hours strain=0.83% R=1.39</p>  <p style="text-align: right;">2.5μm</p>

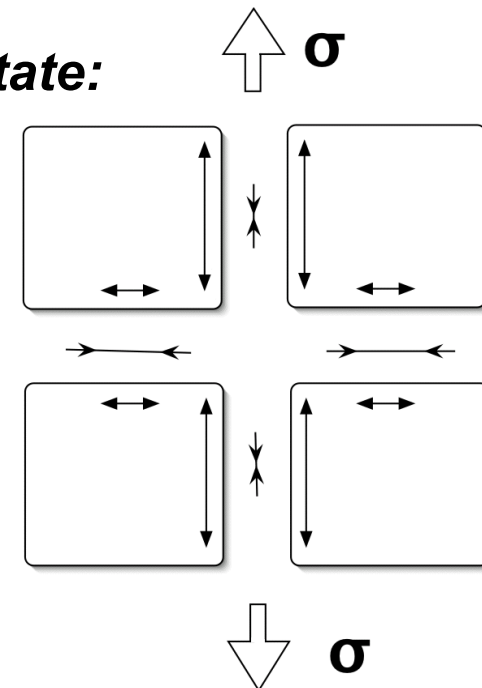
For negative mismatch alloys

$$\delta = \frac{2(a_{\gamma'} - a_{\gamma})}{a_{\gamma'} + a_{\gamma}}$$

Initial State:

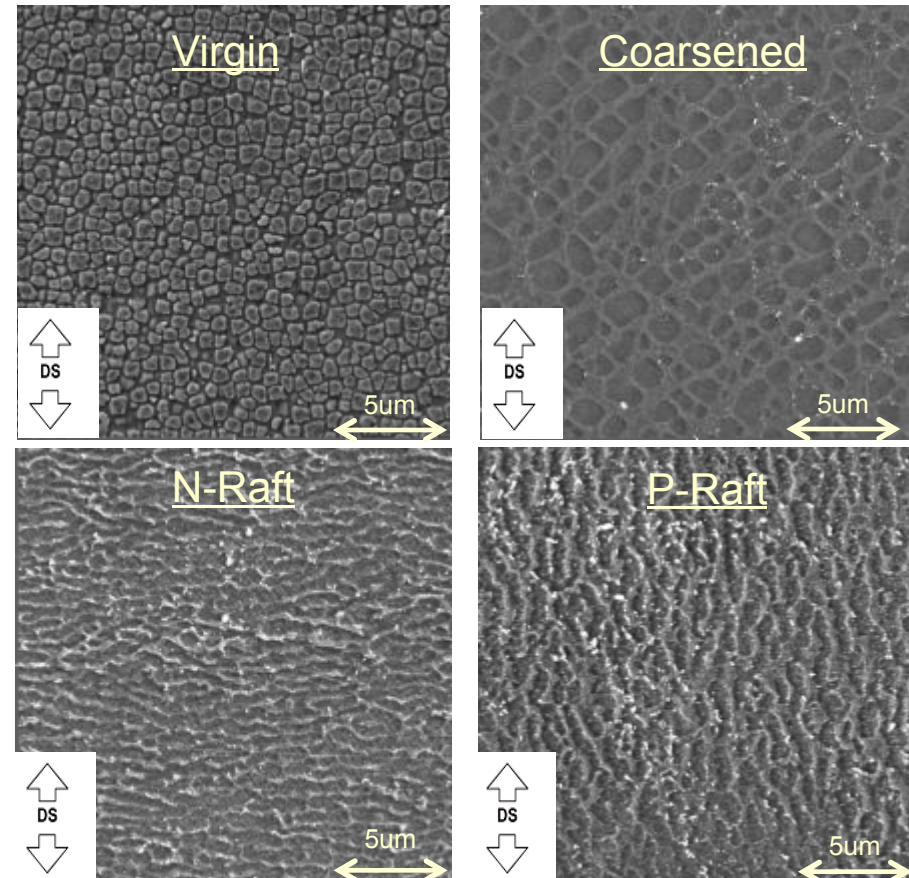
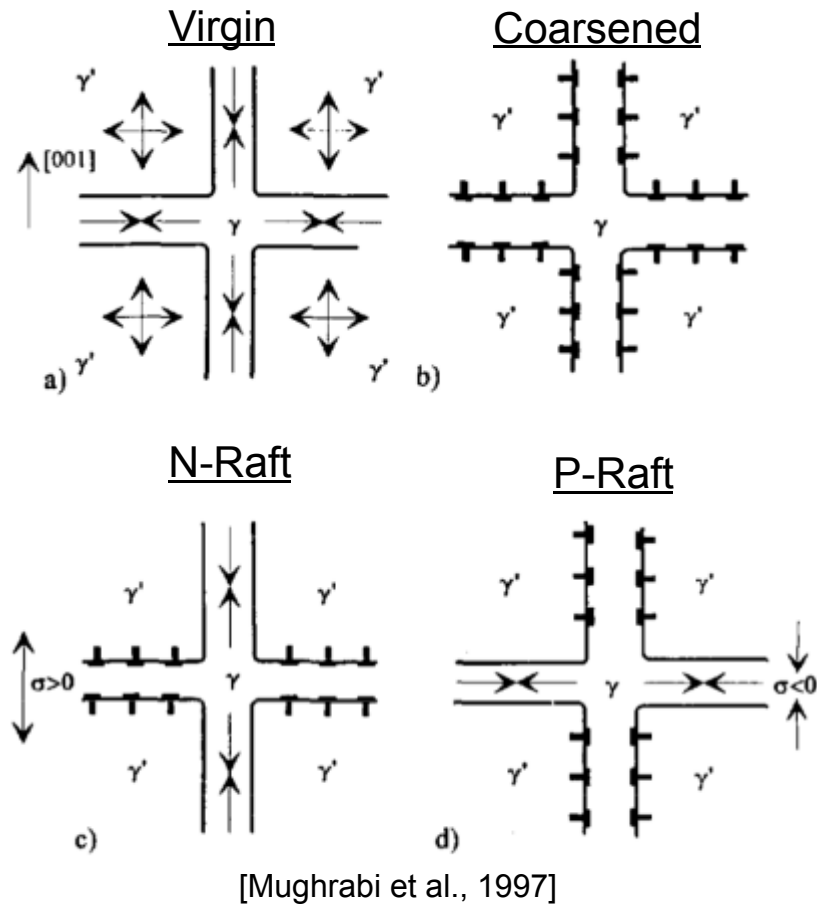


Modified State:



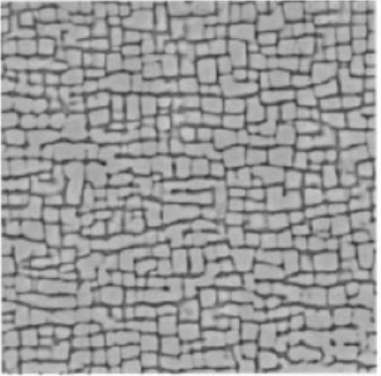
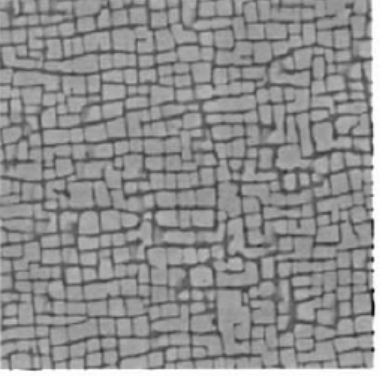
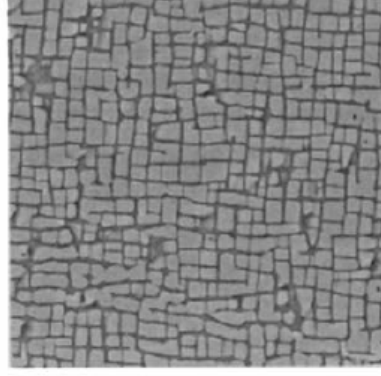
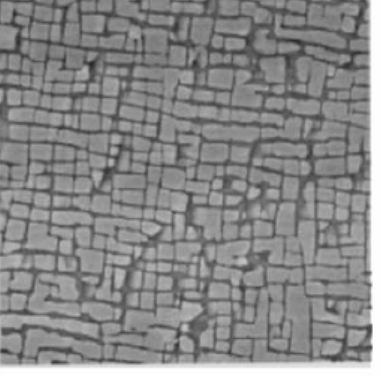
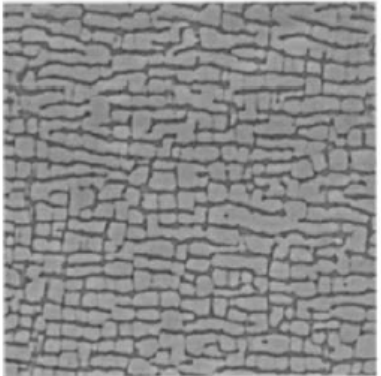
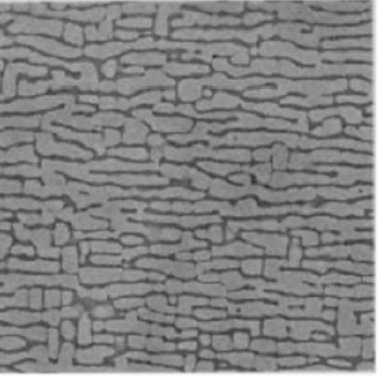
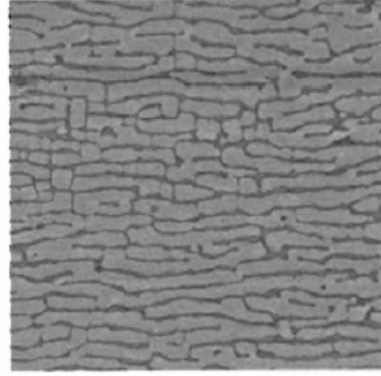
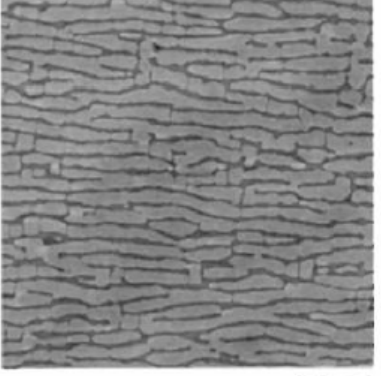
superposition of applied and misfit stresses drive deformation in horizontal channels promoting N-raft formation

- Controlled by difference between the elastic strain energy in the horizontal and vertical γ channels
- Material transport driven by gradient in elastic strain energy density (“elastic” regime when plastic strain $< 0.1\%$)

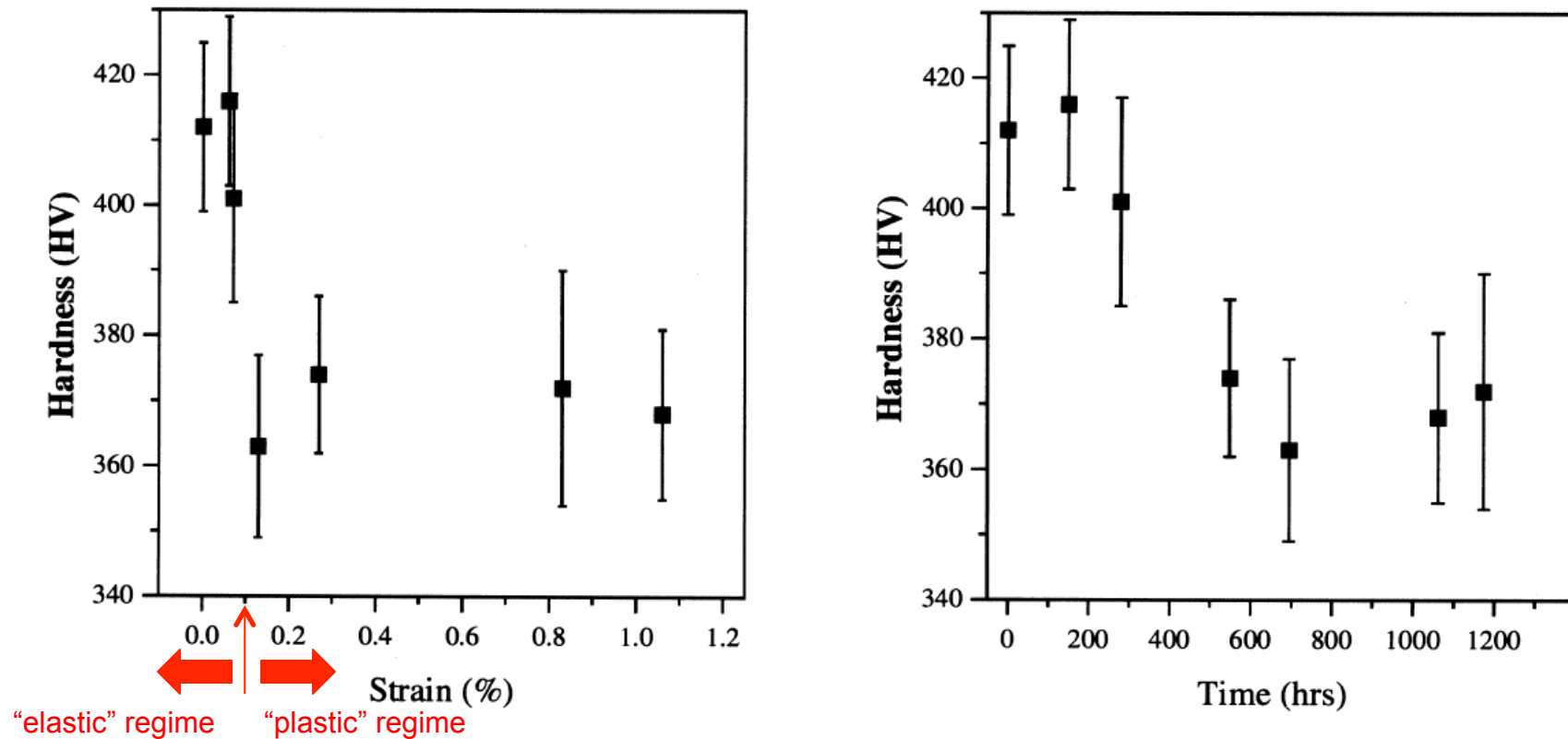


- Dislocations in the horizontal channels (tensile creep case) and their adsorption at the γ/γ' interfaces, resulting in loss of perfect coherency and reduction in elastic misfit strains, is responsible for providing the kinetic path to enable rafting to occur at a reasonable rate.
- Rate in this regime is largely independent of whether the applied stress remains acting or not.

CMSX-4

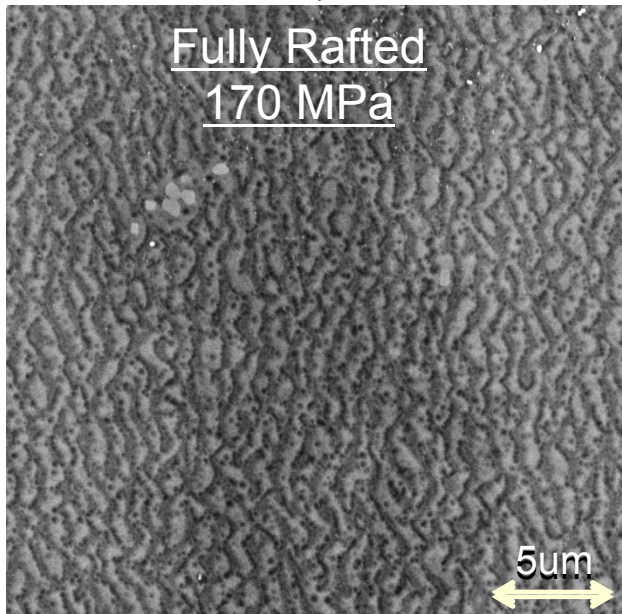
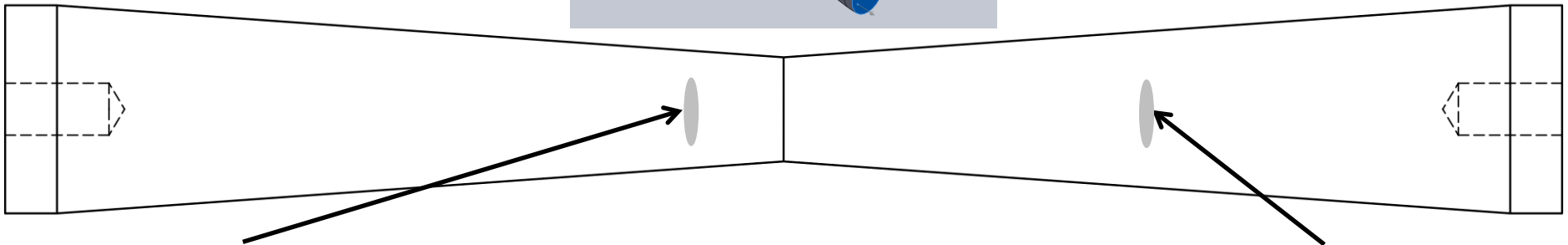
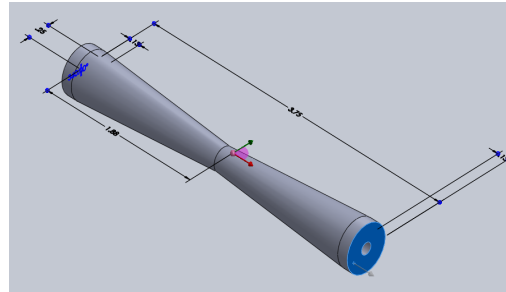
$\sigma=185\text{MPa}$		$\sigma=0\text{ MPa}$		
		time: +100 hrs	time: +300 hrs	time: +600 hrs
B time=280 hrs strain=0.07%				
C time=550 hrs strain=0.27%				

CMSX-4
950°C/185MPa

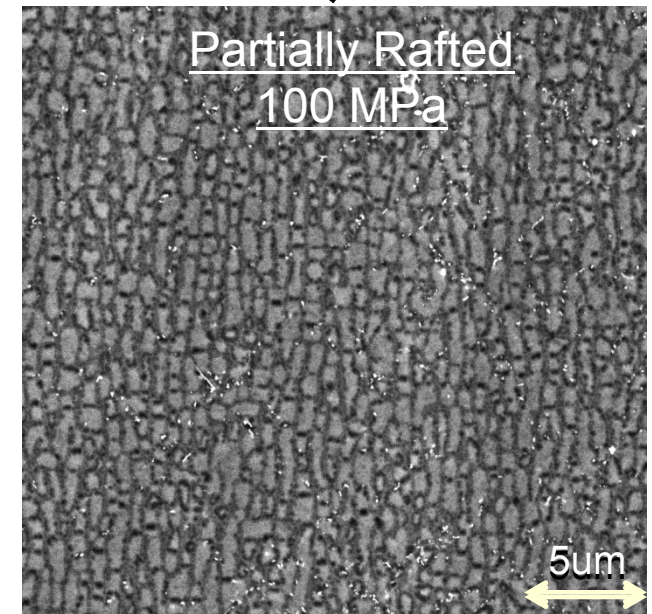


Note: The significant drop in hardness at 0.1% creep strain, representing the threshold strain, is attributed to the loss of coherency of the γ/γ' interfaces because of misfit dislocations present on these interfaces; hence termed "plastic" regime.

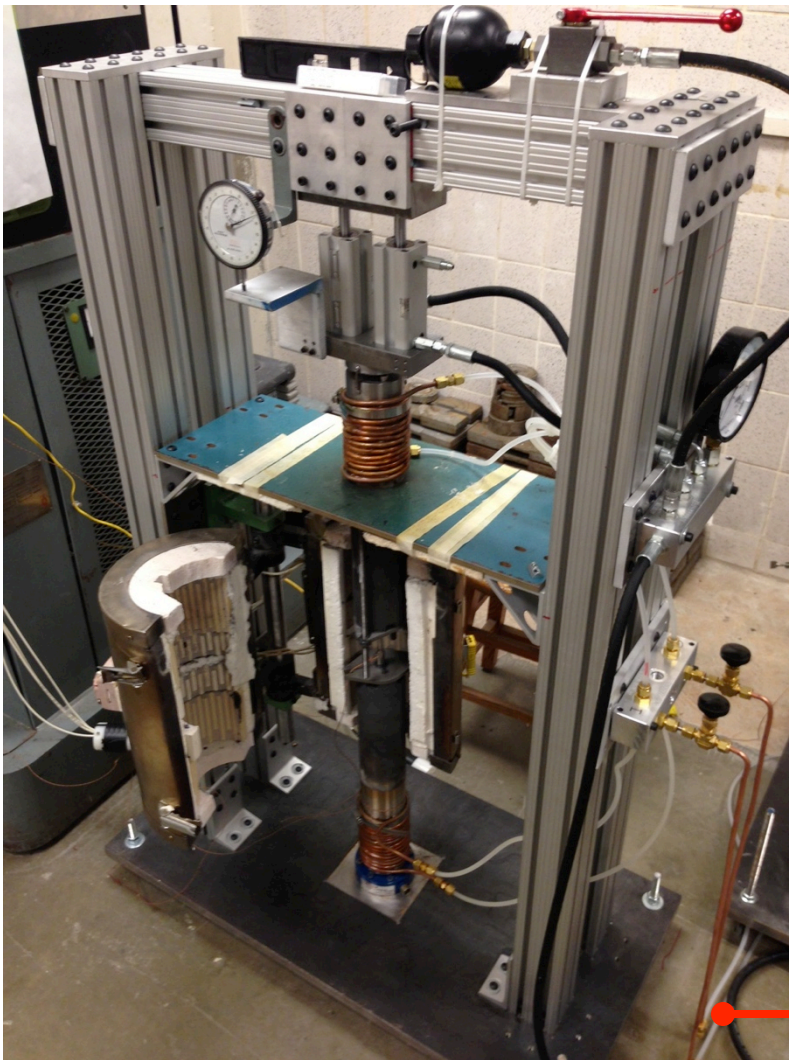
Objective: Obtain kinetic data to predict rafting and coarsening as a function of temperature, stress, microstructure and time



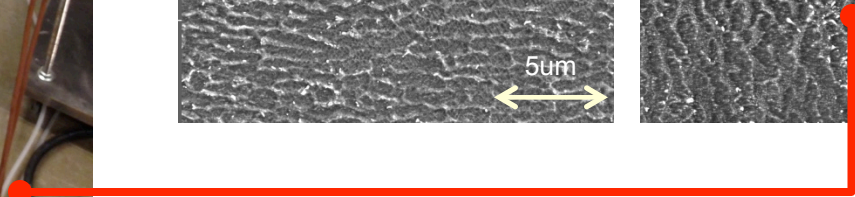
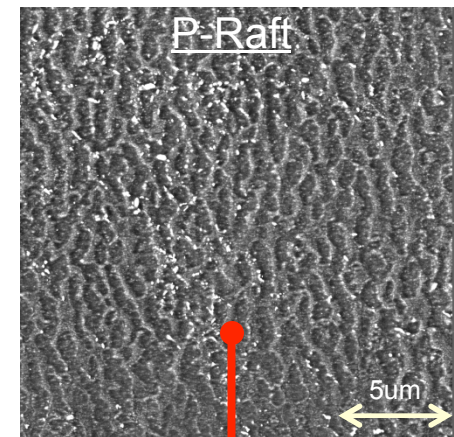
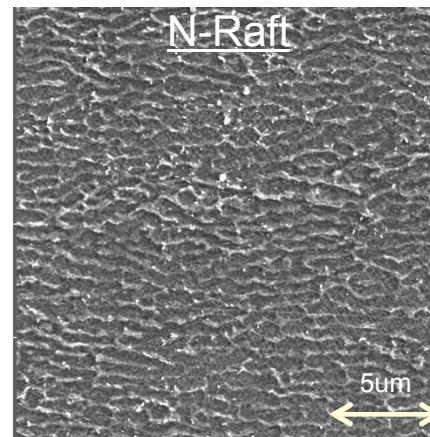
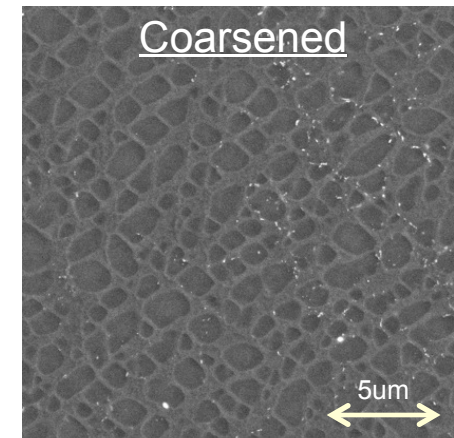
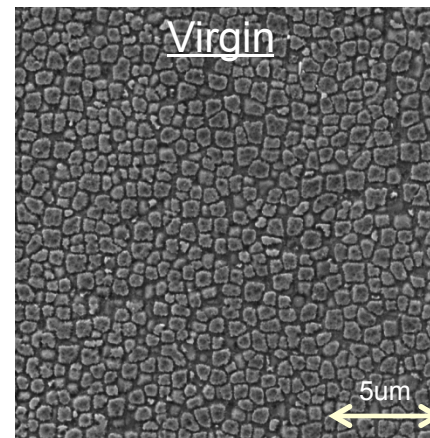
Test conditions
CM247LC-DS
Temperature: 950°C
Force: 1260kN
Time: 500 hrs



Compression Creep Frame

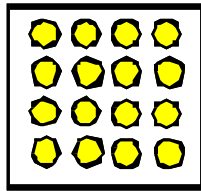


Four Different Microstructures



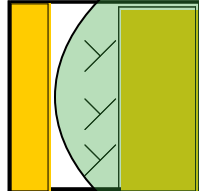
MICROSTRUCTURE-SENSITIVE CRYSTAL VISCOPLASTICITY MODELS

Atomic
(Interfaces,
Cores, Partials)



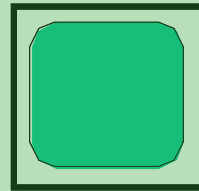
$O(10^{-10} \text{ m})$

Channel
Dislocations



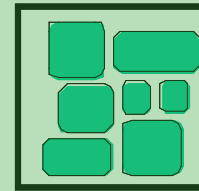
$O(10^{-8} \text{ m})$

Precipitates



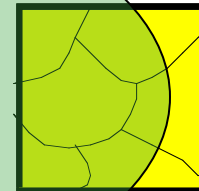
$O(10^{-7} \text{ m})$

Collections of
Precipitates;
GB cracks

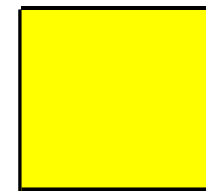


$O(10^{-6} \text{ m})$

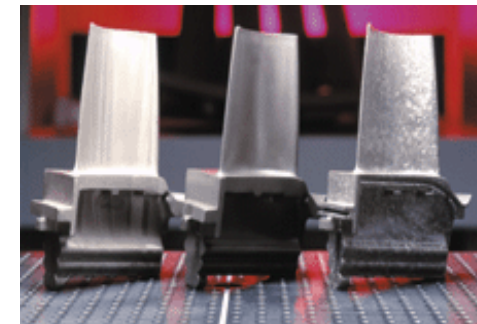
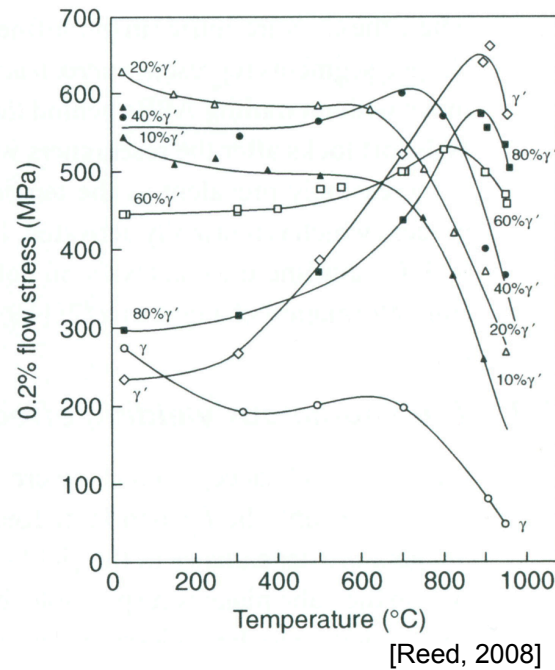
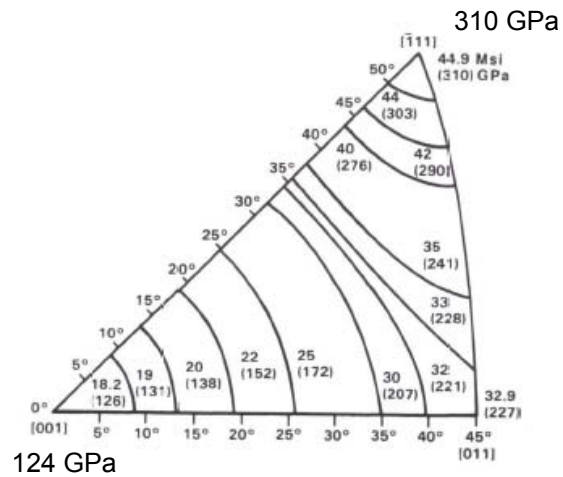
Shear bands
Grains



$O(10^{-5} \text{ m})$



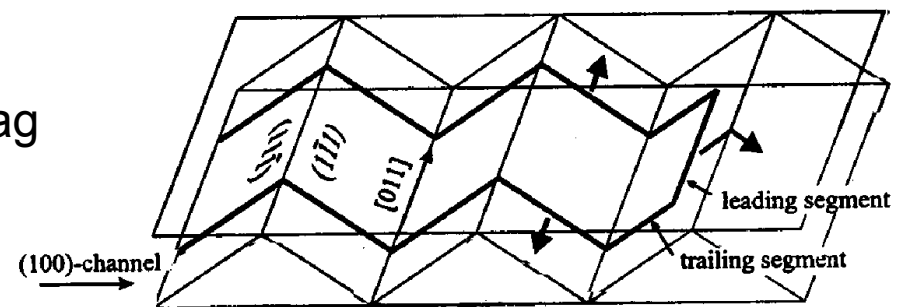
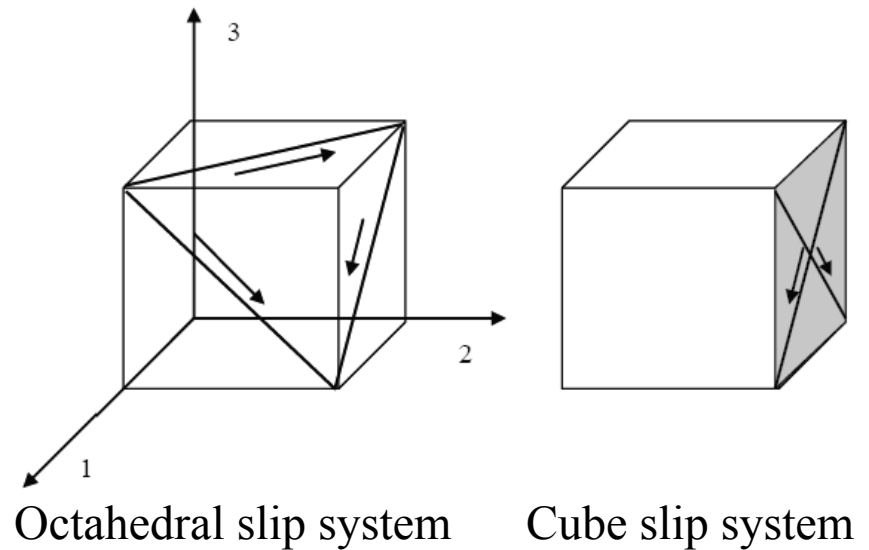
[Shenoy, Tjipowidjojo, and McDowell, 2008]



components

Slip Systems

- Octahedral slip systems
 - Active over entire temperature range
 - [100] loading orientation
 - T/C asymmetry in precipitates
 - Anomalous temperature dependence
- Cube slip systems
 - Active at higher temperatures
 - [111] loading orientation
 - Less T/C asymmetry
 - Macroscopic manifestation of “Zig-Zag mechanism,” [Bettge and Osterle, 1999]



Cube slip [Bettge and Osterle, 1999]

Kinematic relations including temperature dependence

Deformation gradient

$$\mathbf{F} = \frac{\partial \mathbf{x}}{\partial \mathbf{X}} = \mathbf{F}^e \cdot \mathbf{F}^p \cdot \mathbf{F}^\theta$$

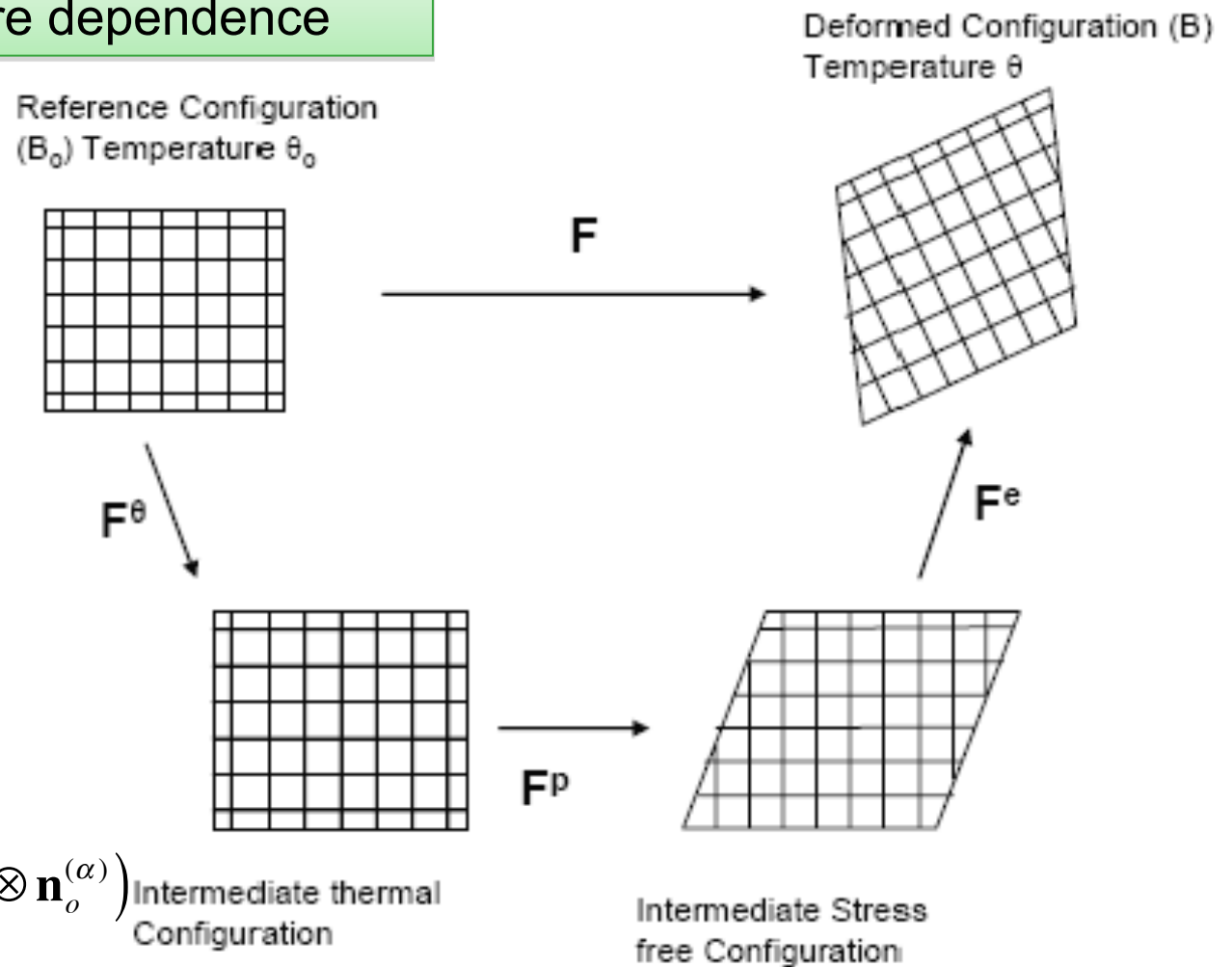
Velocity gradient

$$\mathbf{L} = \dot{\mathbf{F}} \cdot \mathbf{F}^{-1}$$

Macroscopic plastic velocity gradient

$$\mathbf{L}^p = \dot{\mathbf{F}}^p \mathbf{F}^{p^{-1}} = \sum_{\alpha=1}^{N_{slip}} \dot{\gamma}^{(\alpha)} (\mathbf{s}_o^{(\alpha)} \otimes \mathbf{n}_o^{(\alpha)})$$

Intermediate thermal Configuration



$$\mathbf{L}^P = \dot{\mathbf{F}}^P \mathbf{F}^{P-1} = \sum_{\alpha=1}^{N_{slip}} \dot{\gamma}^{(\alpha)} (\mathbf{s}_o^{(\alpha)} \otimes \mathbf{n}_o^{(\alpha)})$$

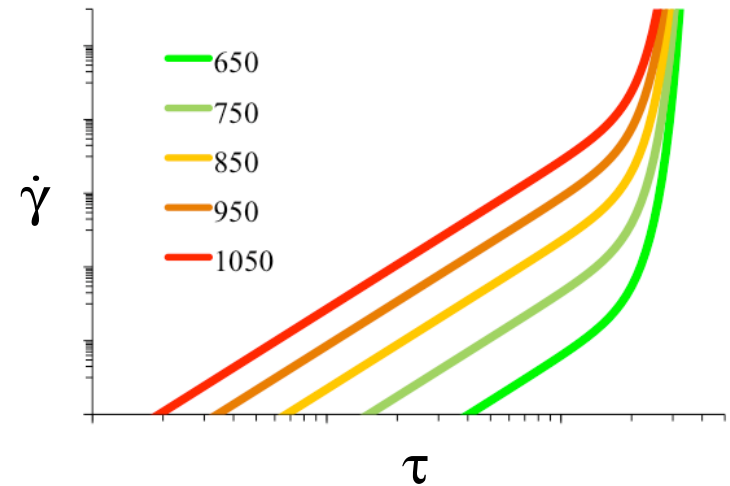
Inelastic Shear Strain Rate

$$\dot{\gamma}^{(\alpha)} = \dot{\gamma}_o \Theta(T) \left\langle \frac{\tau_v^{(\alpha)}}{D^{(\alpha)}} \right\rangle^n \exp \left\{ B_o \left\langle \frac{\tau_v^{(\alpha)}}{D^{(\alpha)}} \right\rangle^{n+1} \right\} \text{sgn}(\tau^\alpha - \chi^\alpha)$$

where

$$\tau_v^{(\alpha)} = |\tau^{(\alpha)} - \chi^{(\alpha)}| - \kappa^{(\alpha)} \frac{\mu}{\mu_o} \quad \text{and} \quad D^{(\alpha)} = D_o \frac{\mu}{\mu_o}$$

$$\Theta(T) = \exp\left(-\frac{Q_o}{RT}\right) \quad \text{for } T \geq \frac{T_m}{2} \quad \Theta(T) = \exp\left(-\frac{2Q_o}{RT} \left[\ln\left(\frac{T_m}{2T}\right) + 1 \right]\right) \quad \text{for } T \leq \frac{T_m}{2}$$



Shenoy, Gordon, McDowell, & Neu (2005)

Creep-fatigue and TMF (temperature-dependent)

$$\dot{\gamma}^{in(\alpha)} = \dot{\gamma}_0 \Theta(T) \left\langle \frac{|\tau^{(\alpha)} - \chi^{(\alpha)}| - \kappa^{(\alpha)}}{D^{(\alpha)}} \right\rangle^n \exp \left\{ B_0 \left\langle \frac{|\tau^{(\alpha)} - \chi^{(\alpha)}| - \kappa^{(\alpha)}}{D^{(\alpha)}} \right\rangle^{n+1} \right\} \text{sgn}(\tau^{(\alpha)} - \chi^{(\alpha)})$$

Shenoy, Tjiptowidjojo, & McDowell (2008)

Creep-fatigue using dislocation-based ISV

$$\dot{\gamma}^{in(\alpha)} = \left[\dot{\gamma}_0 \left\langle \frac{|\tau^{(\alpha)} - \chi^{(\alpha)}| - \kappa^{(\alpha)}}{D^{(\alpha)}} \right\rangle^{n_1} + \dot{\gamma}_1 \left\langle \frac{|\tau^{(\alpha)} - \chi^{(\alpha)}|}{D^{(\alpha)}} \right\rangle^{n_2} \right] \text{sgn}(\tau^{(\alpha)} - \chi^{(\alpha)})$$

MacLachlan, Wright, Gunturi, & Knowles (2001)

Limited to CMSX-4 at 950°C in tertiary regime (stress ≤ 450 MPa) – coupled CVP with damage mechanics

Ma, Dye, & Reed (2008)

Dislocation-based ISV considering primary and tertiary creep regimes (limited to creep of CMSX-4 at 950°C)

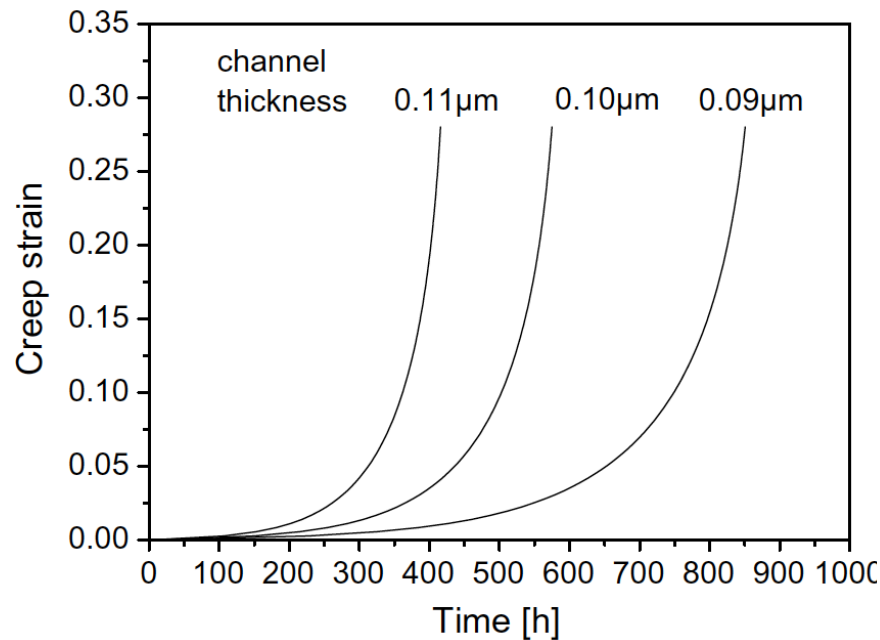
$$\dot{\gamma}_\gamma^{in(\alpha)} = \rho_\gamma^{(\alpha)} b \lambda_\gamma^{(\alpha)} F_{attack} \exp \left\{ \frac{-Q_{slip}^{110} + (|\tau^{(\alpha)} + \tau_{mis}^{(\alpha)}| - \tau_{\gamma pass}^{(\alpha)} - \tau_{oro}^{(\alpha)}) V_{c1}^{(\alpha)}}{kT} \right\} \text{sign}(\tau^{(\alpha)} + \tau_{mis}^{(\alpha)})$$

$$\dot{\gamma}_{L1_2}^{in(\alpha)} = \rho_P^{(\alpha)} b \lambda_{L1_2}^{(\alpha)} F_{attack} \exp \left\{ \frac{-Q_{slip}^{112} + (|\tau^{(\alpha)}| - \tau_{L1_2 pass}^{(\alpha)}) V_{c2}^{(\alpha)}}{kT} \right\} \text{sign}(\tau^{(\alpha)})$$

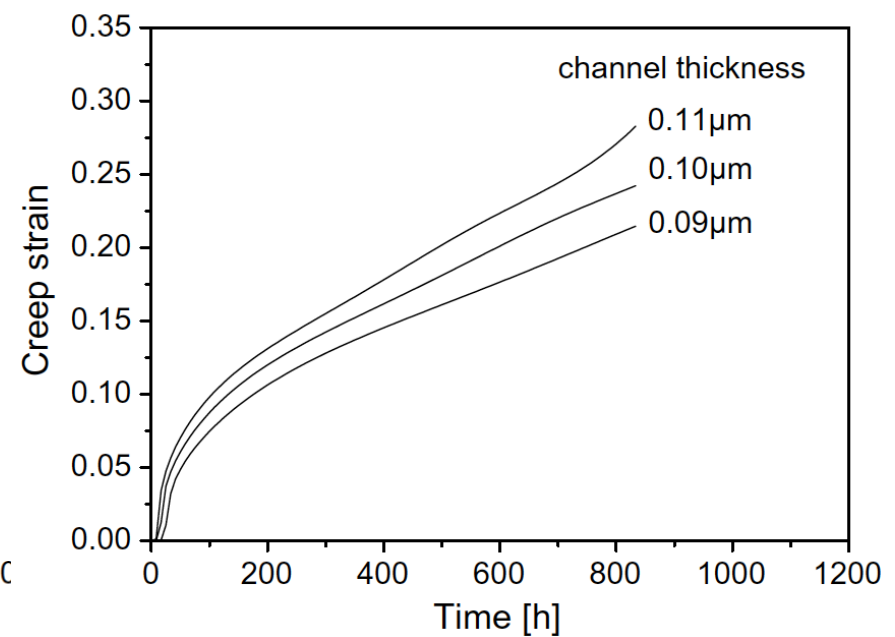
Kirka & Neu (2014)

Added state variables to account for state of aged microstructure in temperature-dependent formulation

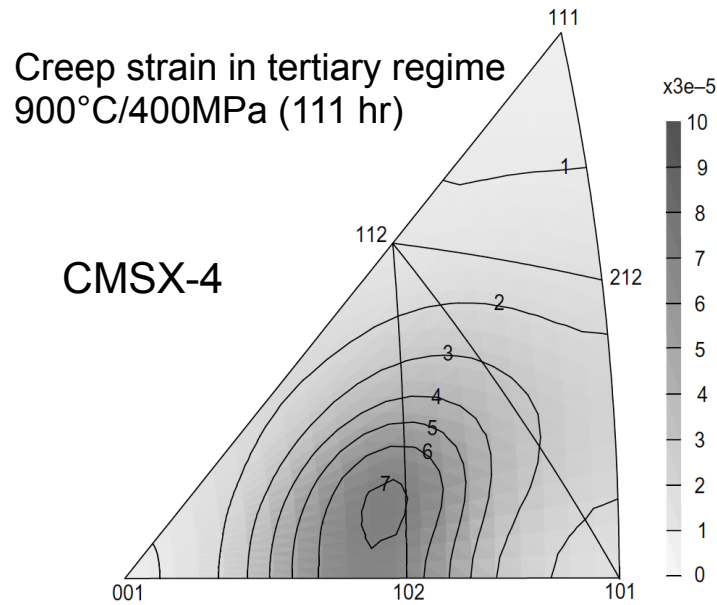
Tertiary creep
950°C/400MPa



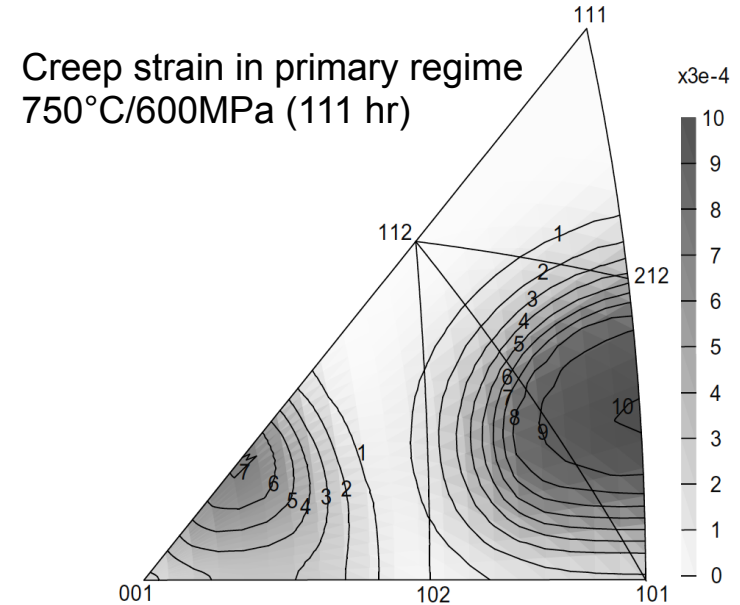
Primary creep
750°C/770MPa



Deformation along [001]
Volume fraction of γ' fixed at 0.7

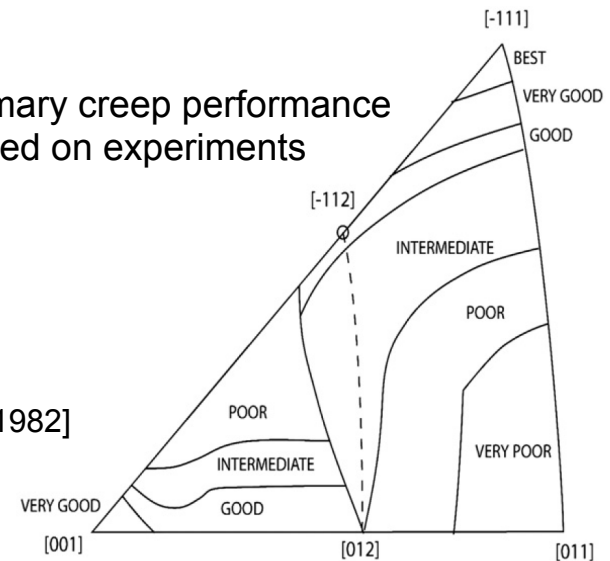


[Ma, Dye, and Reed, 2008]



Primary creep performance based on experiments

[MacKay and Meier, 1982]



- Directional coarsening is roughly a constant volume process
- Stress-free coarsening maintains proportionality between all precipitate/channel dimensions
- Microstructure uniqueness is defined by 2 independent dimensions

$$\text{Rafting: } \dot{w}_i^{raft}(T, \sigma) = - \left(\frac{3Aw_i}{2w_o} \right) \left(\frac{\sigma_i^{dev}}{\sigma_{VM} + \delta} \right) \exp \left(- \frac{Q_{raft} - \sigma_{VM}U(T)}{RT} \right)$$

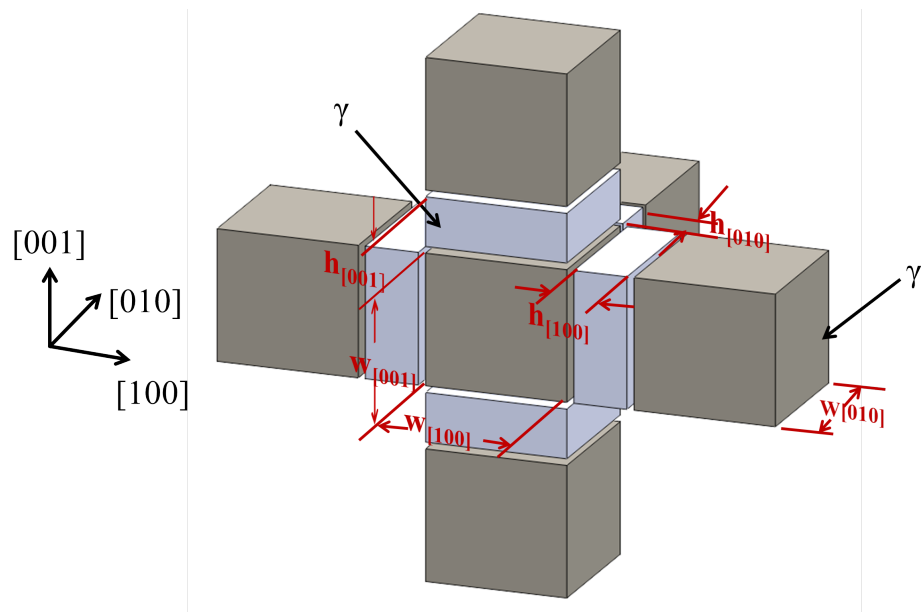
[Tinga, Brekelmans, and Geers, 2009]

$$\text{Isotropic Coarsening: } \dot{w}_i^{coar} = \frac{8K}{3} (w_o^3 + 8Kt)^{-\frac{2}{3}}$$

$$\dot{w}_i = \dot{w}_i^{coar} + \dot{w}_i^{raft}$$

$$\eta = \frac{h_{[001]} - h_{[001]}^o}{h_{[001]}^o}$$

$$\zeta = \frac{h_{[100]} - h_{[100]}^o}{h_{[100]}^o}$$



Prediction of Aging

$$\dot{\omega}_i = \dot{\omega}_i^{coar} + \dot{\omega}_i^{raft}$$

$$\dot{\omega}_i^{coar} = \frac{8K}{3} (\omega_o^3 + 8Kt)^{-2/3}$$

$$r^3 - r_o^3 = K(t - t_o)$$

$$K = \frac{8\sigma DC_o (V_m)^2}{9\nu RT} \quad D = D_o \exp\left(-\frac{Q}{RT}\right)$$

$$\dot{\omega}_i^{raft} = -\left(\frac{3A\omega_i}{2\omega_o}\right) \left(\frac{\sigma_i^{dev}}{\sigma_{VM} + \delta}\right) \exp\left(-\frac{Q_{raft} - \sigma_{VM}U(T)}{RT}\right)$$

Temperature-Dependent Constitutive Models

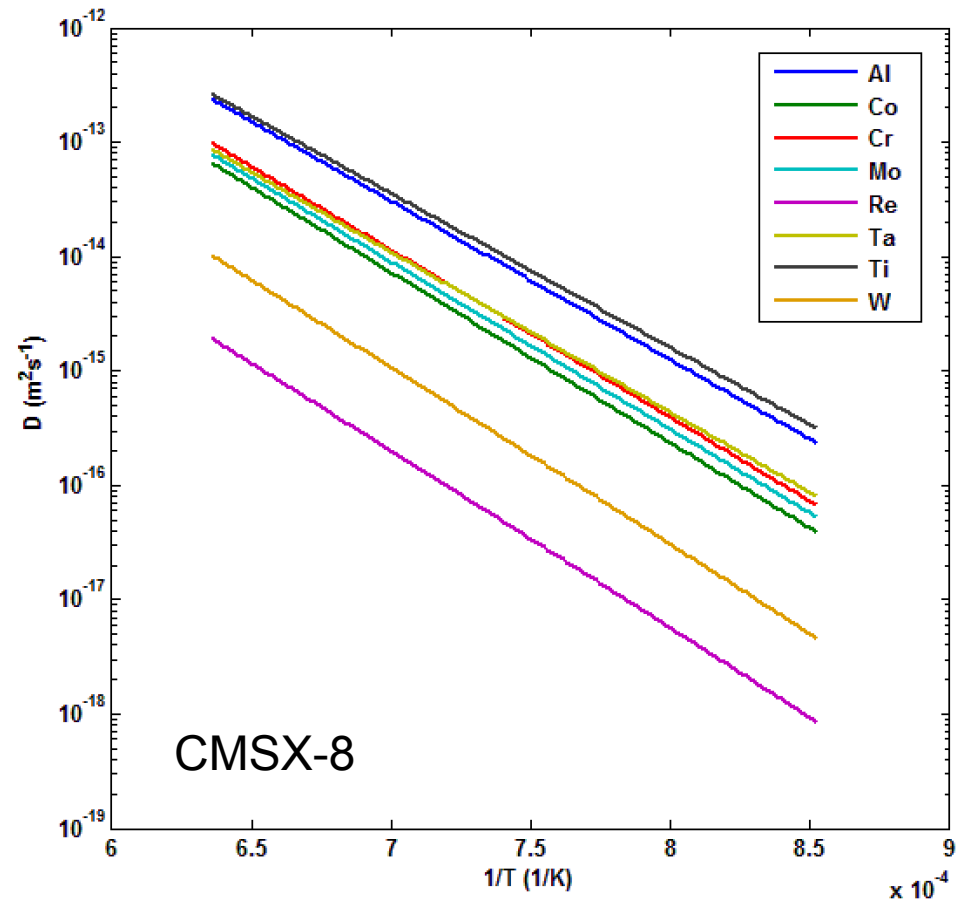
$$\dot{\gamma}^\alpha = \dot{\gamma}_0 \Theta(T) \left\langle \frac{\tau_v^\alpha}{D^\alpha} \right\rangle^n \exp\left\{B_0 \left\langle \frac{\tau_v^\alpha}{D^\alpha} \right\rangle^{n+1}\right\} \text{sgn}(\tau^\alpha - \chi^\alpha)$$

$$\Theta(T) = \exp\left(-\frac{Q_0}{RT}\right) \quad T \geq \frac{T_m}{2}$$

$$\Theta(T) = \exp\left\{-\frac{2Q_0}{RT_m} \left[\ln\left(\frac{T_m}{2T}\right) + 1\right]\right\} \quad T \leq \frac{T_m}{2}$$

Thermo-Calc / DICTRA

Databases: TCNi5 / MOBNI2



Composition Segregation ---- Results

Composition:

CMSX-10		wt%Cr	wt%Co	wt%Mo	wt%W	wt%Ta	wt%Re	wt%Al	wt%Ti	wt%Ni
overall	nominal	2	3	0.4	5	8	6	5.7	0.2	69.7
γ	experiment (dendrite)	3.64	4.95	0.73	9.74	2.34	16.58	1.99	0.06	59.98
	calculation from DICTRA	3.64	6.39	0.67	8.54	0.94	14.2	2.39	0.06	63.17
γ'	experiment (dendrite)	1.29	2.64	0.34	6.96	8.92	4.7	6.93	0.15	68.08
	calculation from DICTRA	1.06	1.07	0.25	2.99	12	1.34	7.59	0.28	73.42
CMSX-8		wt%Cr	wt%Co	wt%Mo	wt%W	wt%Ta	wt%Re	wt%Al	wt%Ti	wt%Ni
	nominal	5.4	10	0.6	8	8	1.5	5.7	0.7	60.1
T=1223K	γ	10.7	20.1	1.3	16.5	0.93	3.47	2.1	0.17	44.73
	γ'	1.6	2.67	0.13	2.05	12.97	0.11	8.28	1.08	71.11
CMSX-4		wt%Cr	wt%Co	wt%Mo	wt%W	wt%Ta	wt%Re	wt%Al	wt%Ti	wt%Ni
	nominal	6.5	10	0.6	6	6	3	5.6	1	61.3
T=1223K	γ	12.15	18.42	1.21	11.57	0.66	6.54	2.16	0.19	47.1
	γ'	1.91	2.95	0.16	1.56	10.37	0.23	8.39	1.72	72.71

- Implement Ma et al. (2008) model
 - add kinematic hardening to improve cyclic loading response
 - CMSX-8 (How much different than CMSX-4? Can it be tied to %Re?)
- Theoretical extensions to embed aging in CVP
- Implementation of CVP model in UMAT/ABAQUS
- Calibration experiments on each microstructure (i.e., artificially aged conditions) of CMSX-8
- Calibration of CVP parameters to CMSX-8
- Validation and demonstration
- Reduced-order formulations for material definition
 - using built in ABAQUS models (uncoupled creep and plasticity; two-layer viscoplasticity)